Interactive Land in E3SM Process-Level Models: Impacts of Land–Atmosphere Coupling in SCM and DP-SCREAM

Peter A. Bogenschutz[1], Yunyan Zhang[1], Hsi-Yen Ma[1], Cheng Tao[1], and Shaocheng Xie[1]

[1]Lawrence Livermore National Laboratory, Livermore, CA

Correspondence: Peter A. Bogenschutz (bogenschutz1@llnl.gov)

Abstract. Process-level modeling is central to diagnosing and improving atmospheric parameterizations in Earth system models, yet continental single-column and convection-permitting process configurations are often run with prescribed surface fluxes, limiting realism and consistency with fully coupled global simulations. Here we develop, document, and demonstrate a reproducible workflow to enable fully interactive land–atmosphere coupling in both the E3SM single-column model (E3SM SCM) and the doubly periodic configuration of SCREAM (DP-SCREAM). The approach leverages a multi-year offline-forced E3SM/ELM integration to provide spun-up land initial conditions and introduces an offline preprocessing method that generates DP-SCREAM–compatible land restart files by extracting and replicating the appropriate ELM grid cell (including its landunit/column/PFT hierarchy) across the doubly periodic domain, avoiding intrusive modifications to ELM I/O. Using daily-initialized two-day hindcast integrations, we apply this framework to two years over GoAmazon and ten years over the Southern Great Plains, and to targeted short process-level cases (CASS and GoAmazon single/double pulse). Interactive land coupling is required to reproduce key near-surface thermodynamic biases characteristic of global coupled simulations, including warm 2-m temperature biases and the elimination of spurious persistent nocturnal fog layers that arise in prescribed-flux configurations. In contrast, prominent cloud and convection process-level biases identified previously (i.e. insufficient deepening of shallow convection, deficits of mid-level congestus, and weak convective organization) are largely insensitive to prescribed versus interactive surface flux treatments, indicating that they are driven primarily by atmospheric model physics and/or dynamics. These results provide both a community-ready capability for coupled land process-level simulations in E3SM and practical guidance on when interactive versus prescribed surface fluxes are appropriate for process-level model evaluation and development.

1 Introduction

Process-level modeling provides a powerful means of evaluating atmosphere parameterizations within earth system models under controlled settings. In the U.S. Department of Energy's Energy Exascale Earth System Model (E3SM; Golaz et al., 2019), two complementary process-level frameworks are widely used: the single-column model (SCM; Bogenschutz et al., 2020), which reduces the global model to a one-dimensional column forced by observations, and the doubly periodic configuration of the Simple Cloud-Resolving E3SM Atmosphere Model (DP-SCREAM; Bogenschutz et al., 2023, 2025b), which extends this approach to convection-permitting scales. Together, these configurations allow direct comparison with observations from field campaigns conducted by the Atmospheric Radiation Measurement (ARM) program (Mather and Voyles, 2013), supporting

evaluation of the model's representation of clouds, precipitation, and boundary-layer processes. ~~Despite their utility, both~~ Previous applications of the E3SM SCM and DP-SCREAM ~~have historically relied on~~ considered here have used prescribed surface fluxes for continental cases~~, limiting the representation of coupled land–atmosphere interactions. This simplification raises important questions about how process-level configurations differ from their~~ . Although useful for isolating atmospheric processes under observational constraints, this treatment suppresses feedbacks between the evolving atmosphere and land surface and can complicate comparison with the coupled parent global model~~, particularly over land~~.

Previous studies have demonstrated both the promise and the limitations of long-term process-level simulations. Tang et al. (2022), for instance, performed multi-year SCM integrations over ARM sites to evaluate the diurnal cycle of precipitation in the tropics and midlatitudes. Their work highlighted the ability of SCM frameworks to isolate persistent model biases, while also underscoring structural limitations in representing coupled land–atmosphere processes. ~~Other modeling efforts have attempted to bridge this gap through simplified interactive landformulations designed for cloud-resolving models (e.g., Lee and Khairoutdinov, 2015), yet no prior study has comprehensively examined the role of interactive land coupling across both SCM and doubly periodic convection-permitting modes within a global Earth system model framework. Addressing this gap is essential, since land~~Interactive land~~–atmosphere feedbacks strongly modulate diurnal cycles, precipitation onset, and boundary-layer evolution (Betts, 2004; Santanello et al., 2018)~~atmosphere coupling is already available in several SCM frameworks. SCAM6 supports an active CLM5 land component and configurable prescribed or model-calculated surface fluxes (Gettelman et al., 2019), while the E3SM SCM likewise supports interactive land, with prescribed fluxes used by default when supplied in the case forcing file (Bogenschutz et al., 2020). Coupled SCM applications include the GABLS3 intercomparison, which examined the influence of land-surface coupling on the diurnal boundary layer (Bosveld et al., 2014), and the ARPEGE–SURFEX configuration of CNRM-CM6-1, used to evaluate land–atmosphere interactions across contrasting land covers (Bernard et al., 2025). Building on this established capability, the present study develops and documents a reproducible initialization and simulation workflow for both E3SM SCM and DP-SCREAM. This includes preparing spun-up E3SM Land Model (ELM) states and mapping the land subgrid hierarchy onto the doubly periodic domain. We then use paired prescribed-flux and interactive-land experiments to assess the influence of coupling on multi-year hindcast statistics and targeted cloud and convection processes.

In this study, we extend the E3SM process-level modeling framework by developing and documenting the ~~technical and scientific steps necessary to couple the~~ initialization and simulation workflow needed to use interactive land coupling in the E3SM SCM and DP-SCREAM configurations~~with the E3SM land model~~. We provide detailed guidance for future users on how to run and configure interactive land simulations, ensuring reproducibility and facilitating broader use of this capability. With this foundation, we present the first set of multi-year hindcast-style simulations with interactive land coupling in E3SM process-level models. Specifically, we conduct two years of simulations at the ARM GoAmazon site (Martin et al., 2017) and a decade of simulations at the ARM Southern Great Plains (SGP) site, following the long-term SCM framework of Tang et al. (2022). Each site is simulated using both E3SM SCM and DP-SCREAM configurations under two surface boundary approaches: prescribed fluxes (traditional) and fully interactive land.

Beyond these long integrations, we also examine shorter process-level case studies drawn from the suite introduced by Bogenschutz et al. (2025b), which were originally designed to expose cloud and convection parameterization biases in global storm-resolving models. These targeted cases enable direct process-level assessment of how interactive land coupling modifies the atmosphere's response, and whether neglecting land–atmosphere interactions risks omitting important processes. By systematically comparing paired prescribed-flux and interactive-land experiments across both E3SM SCM and DP-SCREAM, we create a framework for isolating the contribution of land–atmosphere feedbacks to modeled cloud and precipitation processes.

Our analysis addresses two key scientific questions. First, how do the E3SM SCM and DP-SCREAM configurations compare to each other and to ARM observations when applied to long-term and short-term process studies? Second, to what extent does enabling interactive land coupling alter the fidelity and relevance of process-level simulations? In particular, we ask whether including interactive land allows process-level configurations to more faithfully replicate the biases observed in global E3SM simulations, and what aspects of land–atmosphere feedbacks are missed when fluxes are prescribed. By answering these questions, we demonstrate both the scientific importance and the methodological implications of adding interactive land to E3SM process-level models, and we position this capability as a critical step forward for community use.

2 Model Descriptions

2.1 E3SM Atmosphere Model version 3

The Energy Exascale Earth System Model version 3 (E3SMv3; Xie et al., 2025; Golaz et al., 2026) is the latest generation of the U.S. Department of Energy's fully coupled Earth system model, designed to address mission-relevant science questions. The atmosphere component, the E3SM Atmosphere Model version 3 (EAMv3), builds upon earlier versions by refining parameterizations of convection, turbulence, and microphysics, while adopting a spectral element dynamical core on a cubed-sphere grid. Key physical parameterizations relevant to this study include the ~~CLUBB unified~~ Cloud Layers Unified By Binormals (CLUBB) turbulence and shallow convection scheme (Golaz et al., 2002; Bogenschutz et al., 2013), the enhanced Zhang–McFarlane deep convection scheme (Zhang and McFarlane, 1995; Song et al., 2023, 2025), and the updated Predicted Particle Properties (P3) microphysics scheme for stratiform clouds (Morrison and Milbrandt, 2015; Shan et al., 2023). More details about cloud microphysics and deep convection used in EAMv3 are described in Terai et al. (2025). The land component is represented by ELM, which exchanges surface fluxes of heat, moisture, and momentum with the atmospheric column.

2.1.1 E3SM Single Column Model

The E3SM single-column model (E3SM SCM) reduces the three-dimensional EAMv3 to a one-dimensional vertical column, forced by prescribed large-scale tendencies derived from observations or reanalyses. This framework enables targeted evaluation of parameterization behavior against in situ and remote-sensing measurements while maintaining consistency with the full model's physics suite (Bogenschutz et al., 2020). The E3SM SCM has been widely used to isolate cloud and precipitation biases, as well as to evaluate boundary-layer and convection schemes under controlled conditions. Traditionally, SCM simula-

tions prescribe surface fluxes to isolate atmospheric processes, but this study extends the capability to allow fully interactive land–atmosphere coupling.

2.2 SCREAM version 1

The Simple Cloud-Resolving E3SM Atmosphere Model version 1 (SCREAMv1; Donahue et al., 2024) is the atmosphere configuration of E3SMv3 designed for global storm-resolving simulations at horizontal grid spacings of 3 km or finer. SCREAMv1 replaces traditional convection parameterizations with explicit representation of deep convection, while retaining parameterizations for turbulence, shallow convection, and microphysics. The model employs the P3 single-moment microphysics scheme (Morrison et al., 2015), a scale-aware implementation of ~~SHOC~~ the Simplified Higher-Order Closure (SHOC) for boundary-layer turbulence and shallow clouds (Bogenschutz and Krueger, 2013), and a non-hydrostatic spectral element dynamical core optimized for ~~GPU-accelerated~~ graphics processing unit (GPU)-accelerated architectures. SCREAMv1 is coupled to ELM, enabling the explicit resolution of cloud–precipitation systems while maintaining fully interactive land–atmosphere exchanges.

2.2.1 Doubly Periodic SCREAMv1

The doubly periodic configuration of SCREAMv1 (DP-SCREAMv1) extends the process-level modeling capability of E3SM to the convection-permitting scale by imposing periodic lateral boundary conditions on a limited-area SCREAMv1 domain. This framework allows for controlled simulations of cloud systems under observed large-scale forcings at resolutions typical of global GSRMs and large-eddy simulations (DP-SCREAM; Bogenschutz et al., 2023, 2025b). DP-SCREAMv1 is fully consistent with the global SCREAMv1 physics suite, including turbulence, shallow convection, and microphysics parameterizations. Previous studies have demonstrated its ability to reproduce observed cloud processes and to expose structural model biases in a computationally efficient manner. In this work, we extend DP-SCREAMv1 to operate with an interactive land model.

2.3 ELM Land Model

The land surface in our simulations is represented by the E3SM Land Model version 2 (ELMv2; Golaz et al., 2022), which simulates the exchange of energy, water, and momentum between the land surface and atmosphere. ELMv2 represents hydrologic and thermodynamic processes within vegetation, snow, and soil across multiple land cover types, including vegetated surfaces, bare soil, lakes, glaciers, and urban regions. Vegetation properties are prescribed from satellite-derived datasets, including leaf area index, while land cover distributions are specified from observationally based land-use datasets. Relative to earlier versions, ELMv2 includes updates to vegetation representation and incorporates the Snow, Ice, and Aerosol Radiative model with Adding-Doubling solver (SNICAR-AD~~snow radiative transfer model~~), which improves the treatment of snow albedo and snow–radiation interactions. Through these processes, ELMv2 provides interactive surface fluxes of heat, moisture, and momentum that influence the evolution of the atmospheric boundary layer and cloud fields.

3 ~~Interactive Land Model Capability in SCM and DP-SCREAM~~

2.1 System for Atmospheric Modeling

The System for Atmospheric Modeling (SAM; Khairoutdinov and Randall, 2003) provides the large-eddy simulation (LES) reference for the CASS and GoAmazon process-level cases. These reference simulations resolve the dominant turbulent eddies and convective structures, with subgrid turbulence represented by a 1.5-order turbulent kinetic energy closure and cloud microphysics by a single-moment bulk scheme. We use the CASS reference of Zhang et al. (2017) and the GoAmazon single- and double-pulse references of Tian and Zhang (2025), following the configurations summarized by Bogenschutz et al. (2025b) . The CASS reference uses 50-m horizontal spacing on a $512 \times 512 \times 156$ grid, whereas the GoAmazon references use 250-m horizontal spacing on a $512 \times 512 \times 266$ grid. These prescribed-flux LES references provide a common benchmark for evaluating cloud and convection behavior in the DP-SCREAM experiments; they are not additional interactive-land sensitivity experiments.

3 Interactive Land Model Capability in E3SM SCM and DP-SCREAM

The capability to couple an interactive land model has long existed in both the E3SM ~~Single Column Model (SCM)~~ SCM and the doubly periodic SCREAM (DP-SCREAM) configurations. In practice, however, most simulations have been performed using prescribed surface fluxes. In ~~such cases, the land model technically runs in the background, but its prognostic outputs~~ the prescribed-flux configuration, ELM continues to run, but the surface sensible and latent heat fluxes supplied to the atmosphere are overwritten by the prescribed ~~flux data. The~~ values. This replacement applies to turbulent heat and moisture exchange with the atmosphere, rather than prescribing the ground heat flux, which represents conductive heat exchange within the land surface. The imposed turbulent fluxes cannot adjust to the evolving simulated near-surface temperature and humidity, so their consistency with the simulated surface and atmospheric energy budgets is not guaranteed. However, the present analysis does not isolate the contributions of ground heat exchange, radiative cooling, and turbulent heat transport to the nighttime cold bias and associated fog; establishing their relative roles requires a dedicated energy-budget analysis. The primary limitation preventing interactive land coupling has been the need for realistic initial land conditions. Running with a "cold start" is scientifically unjustified, as the land model typically requires multiple years, often five or more, of spin-up to achieve equilibrium in soil moisture and temperature (Lawrence et al., 2011; Golaz et al., 2019; Lombardozzi et al., 2020). Given that E3SM SCM and DP-SCREAM simulations generally span only a few days to a few months, using a non–spun-up land state would lead to unrealistic surface energy and moisture budgets.

To address this issue, the models were modified to ingest a spun-up land state generated from a fully coupled E3SM simulation (see Section 4.3 for details). For the E3SM SCM, this functionality was already largely implemented and required only minor code modifications to correctly map the desired land column from the global spun-up dataset. In contrast, enabling the same capability in DP-SCREAM proved substantially more challenging, requiring the development of new procedures to correctly initialize and interface the land model with the doubly periodic configuration.

Unlike the ~~single-column model (SCM)~~E3SM SCM, the doubly periodic SCREAM (DP-SCREAM) configuration is built on an unstructured horizontal mesh that does not directly correspond to the structured grid used by the global E3SM Land Model (ELM). Incorporating an interactive land surface therefore posed significant technical challenges. To initialize DP-SCREAM with a spun-up land state, the model must first identify the ELM grid cell that most closely matches the latitude and longitude of the target domain. Once identified, all associated land subcomponents, including landunits, columns, and plant functional types (PFTs), must be propagated across the doubly periodic grid. These elements form the hierarchical structure of ELM, where each grid cell contains multiple landunits (e.g., vegetated, bare soil, or lake), each landunit may contain several columns (representing independent soil columns or snowpacks), and each column may host several PFTs. Properly reproducing these relationships within the DP-SCREAM framework would require extensive modification of ELM's parallel ~~I~~input/~~O~~ output (PIO) routines to re-map, replicate, and write consistent indices for each of these subgrid entities. Implementing such capability natively in ELM would have been complex, error-prone, and disruptive to the core I/O framework.

To avoid major code restructuring, we instead developed an offline Python preprocessing script that generates DP-SCREAM–compatible land initial condition files from an existing spun-up ELM restart dataset. The script reads a user-specified ELM restart file from a lower-resolution E3SM simulation, locates the grid cell nearest the latitude and longitude of the desired DP-SCREAM domain, and extracts all variables associated with that grid cell and its hierarchical subcomponents (landunits, columns, and PFTs). These fields are then replicated across the full doubly periodic grid according to the desired domain geometry (specified by num_ne_x and num_ne_y) and written to new NetCDF files with consistent dimensions and metadata. This replication is used only to initialize the simulation; once the model begins integrating, ELM is run interactively on the same high-resolution grid as DP-SCREAM, allowing land states and surface fluxes to evolve independently at each grid cell. This approach allows DP-SCREAM to start from a physically consistent, spun-up land state without requiring any modification to ELM source code, providing a flexible and reproducible mechanism for initializing interactive land simulations. A copy of this script can be found in Bogenschutz (2026).

4 Experiment Design

To investigate the influence of surface flux representation in process-level configurations, we performed two complementary sets of simulations: long-term runs to evaluate the impact of prescribed versus interactive fluxes on climatological biases, and shorter-duration experiments to assess their importance for reproducing process-level variability.

Table 1 summarizes the model configurations, cases, spatial resolutions, domains, and purposes of the experiments and reference simulations.

4.1 Long Term Forcing Simulations

Two-year simulations were performed for both the E3SM ~~Single Column Model (SCM)~~ SCM and the doubly periodic SCREAM (DP-SCREAM) using continuous large-scale forcing derived from the ARM GoAmazon field campaign (Tang et al., 2016) covering the period from January 2014 to December 2015. In addition, 10-year simulations were performed for

Table 1. Summary of experiments and reference simulations. Resolution denotes horizontal grid spacing unless a grid identifier is given. Each atmospheric E3SM experiment is run with both prescribed surface fluxes and interactive land. Long-term experiments use daily initialized two-day hindcasts, retaining only day two. The SAM LES references use prescribed surface fluxes and the configurations described in Bogenschutz et al. (2025b).

Model	Case or period	Resolution	Horizontal domain	Purpose
Offline ELM	January 2001–December 2015	ne30pg2	Global	Generate spun-up land restart files under ERA5 forcing
E3SM SCM	GoAmazon, 2014–2015; SGP, 2006–2015	Single column	One column per site	Evaluate long-term atmospheric and surface biases and sensitivity to land coupling
DP-SCREAM	GoAmazon, 2014–2015; SGP, 2006–2015	3.25 km	200×200 km	Evaluate long-term convection-permitting behavior and sensitivity to land coupling
DP-SCREAM	CASS composite	3.25 km; 100 m	50×50 km	Evaluate shallow cumulus and sensitivity to resolution and land coupling
DP-SCREAM	GoAmazon single pulse, 5 October 2014	3.25 km; 250 m	200×200 km	Evaluate shallow-to-deep transition and sensitivity to resolution and land coupling
DP-SCREAM	GoAmazon double pulse, 26 August 2015	3.25 km; 250 m	200×200 km	Evaluate repeated convective development and sensitivity to resolution and land coupling
SAM LES	CASS composite	50 m	25.6×25.6 km	Reference for shallow-cumulus evolution
SAM LES	GoAmazon single- and double-pulse cases	250 m	128×128 km	Reference for shallow-to-deep convective transitions

each configuration at the ARM Southern Great Plains (SGP) site spanning January 2006 through December 2015. The DP-SCREAM simulations were conducted over a 200 km × 200 km domain with 3.25 km horizontal grid spacing, using the same time-step settings as the global SCREAM configuration (Donahue et al., 2024). Both the E3SM SCM and DP-SCREAM were run using two surface configurations: (1) prescribed surface fluxes obtained from the ARM variational analysis (Zhang et al., 2001; Xie et al., 2004) and (2) fully interactive surface fluxes.

To minimize model drift and prevent the accumulation of errors, all simulations were conducted in hindcast mode following the methodology of Tang et al. (2022). Specifically, each configuration was initialized daily at 00 UTC and integrated forward for two simulation days, with only the second day retained for analysis. The first simulation day serves as a spin-up period, allowing the model physics to adjust to the imposed large-scale forcing and initial conditions, while reducing initialization artifacts. No nudging was applied to temperature or moisture fields. Compared to traditional SCM experiment protocols, such as free-running (e.g., Ghan et al., 2000) or nudged simulations, the two-day hindcast approach constrains large-scale conditions sufficiently to prevent divergence from observations while still reproducing the same intrinsic model biases as in global simulations.

Each 10-year hindcast simulation set for DP-SCREAM corresponds to roughly 20 years of total simulated time at convection-permitting resolution. This computationally demanding task was made feasible by leveraging GPU acceleration (Bogenschutz et al., 2025a). Each DP-SCREAM hindcast was executed on a single GPU node of the ~~NERSC~~ National Energy Research Scientific Computing Center (NERSC) Perlmutter system, where a two-day simulation completed in under four minutes, approximately eight times faster than on ~~CPU~~ central processing unit (CPU) nodes. Although the hindcast setup requires greater infrastructure to manage and submit large numbers of short jobs, the overall computational workflow is highly efficient. The short wall-clock times allow many runs to execute in parallel with minimal queue wait time, enabling the complete set of 10-year DP-SCREAM hindcasts to finish within 24 hours of job submission.

4.2 Process Level Cases

Two process-level cases are used in this study to evaluate the DP-SCREAM configurations: the Continental Active Surface-forced Shallow-cumulus (CASS, Zhang et al., 2017) case and the GoAmazon shallow-to-deep cumulus transition cases (Tian and Zhang, 2025). The CASS case represents the composite behavior of fair-weather shallow cumulus observed at the ARM Southern Great Plains site and is designed to capture the diurnal evolution of continental shallow convection forced by surface heating. The GoAmazon cases, derived from the ARM GoAmazon field campaign, characterize the transition from shallow to deep convection over the Amazon basin, including both a “single-pulse” and “double-pulse” event representative of different convective regimes. Together, these cases provide a complementary test bed spanning shallow, transitional, and deep convective processes under distinct continental and tropical environments. Each case is run following the prescribed large-scale forcing and surface conditions described in Bogenschutz et al. (2025b), which provides a detailed description of the experimental setup, forcings, and simulation protocols. In this work we run both of the cases with prescribed and interactive surface fluxes for each configuration. In addition to the default 3-km DP-SCREAM simulations, each case is also performed at higher resolution: 100 m for the CASS case and 250 m for the GoAmazon cases.

4.3 Land Model Spin-Up

To generate spun-up land initial conditions for use in the E3SM SCM and DP-SCREAM configurations, we performed a dedicated E3SMv3 simulation using the IELM ~~compset,~~ component set (compset), an offline configuration in which the ~~atmosphere is prescribed with ERA5 reanalysis forcing~~E3SM Land Model is active and atmospheric forcing is supplied by a data atmosphere rather than a prognostic atmospheric model. Here, the forcing is taken from the fifth-generation European Centre for Medium-Range Weather Forecasts atmospheric reanalysis (ERA5; Hersbach et al. (2020)). The simulation was conducted ~~at ne30pg2 horizontal resolution using the~~ on the `ne30pg2` cubed-sphere grid, where `ne30` denotes 30×30 spectral elements on each of the six cube faces and `pg2` denotes 2×2 finite-volume physics cells per element; this grid configuration has a nominal horizontal resolution of approximately 100×100 km at the equator. The simulation used the E3SM maintenance branch version 3.0.2 ~~,~~ and was integrated continuously from January 2001 through December 2015. Monthly ELM restart files were archived throughout the integration and subsequently used to initialize the land component in the process-level experiments described in this study. For the long-term forcing simulations at the GoAmazon and SGP sites, land restart files corresponding to the month and year of each campaign were selected for both E3SM SCM and DP-SCREAM cases to ensure consistency with observed surface conditions. To assess sensitivity to restart frequency, we also performed a one-year GoAmazon simulation initialized with daily restart files, and found no significant differences relative to runs initialized from the corresponding monthly restarts, confirming that the monthly restart frequency is sufficient for initializing the land surface in these configurations.

For the process-level simulations, the single- and double-pulse GoAmazon cases use land initial conditions corresponding to the exact initialization time of each case: 05 October 2014 at 12 UTC for the single-pulse case and 26 August 2015 at 12 UTC for the double-pulse case. The CASS case, by contrast, represents a composite of 76 "golden" shallow cumulus days. Its land initial condition file is constructed by averaging a subset of approximately 30 daily initial condition files associated with this case, all initialized at 12 UTC.

5 Results

The results are organized as follows. Section 5.1 presents findings from the long-term simulations, beginning with a two-year integration over the GoAmazon site and followed by a ten-year simulation at the Southern Great Plains (SGP) site. This section focuses on (1) the skill of DP-SCREAM and E3SM ~~single-column model (SCM)~~ SCM simulations and (2) the role of land–atmosphere coupling in reproducing biases observed in the global model. Section 5.2 then examines process-level behavior, first through a single shallow cumulus case and subsequently through two realizations of the transition from shallow to deep convection. This section considers only DP-SCREAM simulations applied to a set of cases previously shown to expose process-level biases when surface fluxes are prescribed (Bogenschutz et al., 2025b). Here, we evaluate whether or not neglecting land–atmosphere coupling renders these cases an inadequate proxy for reproducing model biases.

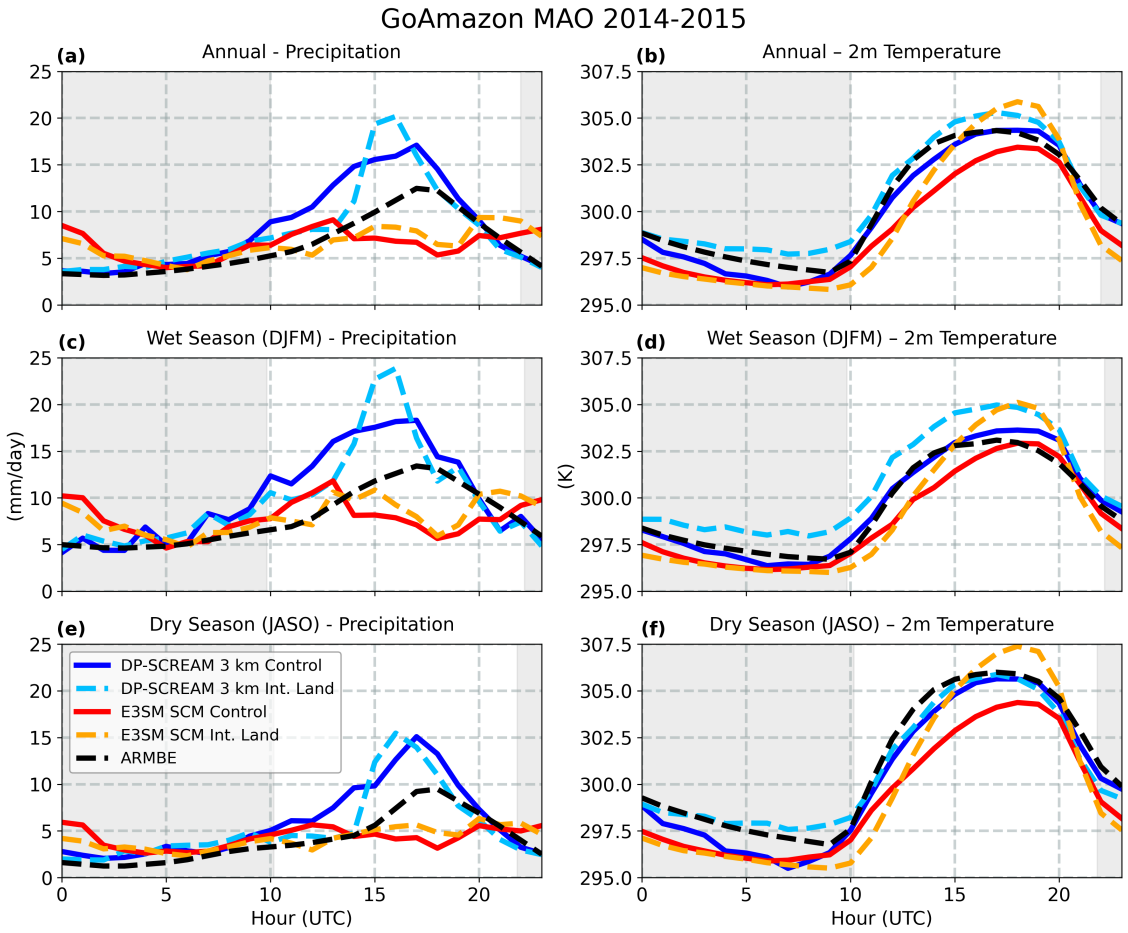

Figure 1. Diurnal cycle composites for the period 1 January 2014 to 31 December 2015 at the GoAmazon MAO site for (left column) precipitation rate and (right column) 2-m air temperature from ARM best estimate (ARMBE, Xie et al., 2010) observations, the E3SM ~~single-column model~~SCM, and DP-SCREAM at 3-km horizontal resolution. For the E3SM SCM and DP-SCREAM simulations, solid curves denote the control configuration with prescribed surface fluxes, while dashed curves denote simulations with interactive surface fluxes. The top row shows annual composites, the middle row shows composites for the local wet season (December–March), and the bottom row shows composites for the local dry season (July–October). Shading denotes the averaged nighttime hours for this location. Time is shown in UTC; the model composites include only the second day of each daily initialized two-day hindcast.

5.1 Long Term Forcing Simulations

5.1.1 Amazon

As a first long-term test case, we analyze two years of hindcast simulations over the GoAmazon region to examine the role of surface–atmosphere coupling in shaping persistent thermodynamic and precipitation biases in convection-permitting simula-

tions. Figure 1 shows composites of precipitation and near-surface (2-m) air temperature, including annual-mean composites as well as seasonal composites for the wet season (December–March; DJFM) and dry season (July–October; JASO).

For both process-level configurations with interactive land coupling, the annual and wet-season composites exhibit a pronounced daytime warm bias, with the largest amplitude occurring during the wet season. In addition to this daytime error, the DP-SCREAM configuration systematically develops a positive nighttime 2-m temperature bias, whereas the E3SM SCM simulations do not exhibit a comparable nocturnal warming. Consistent with global SCREAMv1 results (Donahue et al., 2024), this nighttime warm bias is absent when surface fluxes are prescribed, indicating that interactive land coupling is a necessary condition for reproducing the sign and diurnal structure of the temperature biases seen in the global model. Although the magnitude of the bias in these hindcast simulations is smaller than in the global configuration, likely because the hindcast framework limits the accumulation of slow land–atmosphere feedbacks, the DP-SCREAM simulations nonetheless capture the correct phase and structure of the error. The absence of a comparable nighttime bias in E3SM SCM suggests that differences in boundary-layer turbulence or land–atmosphere coupling strength act to damp nocturnal temperature errors in that model.

It is notable that both E3SM SCM and DP-SCREAM simulations employing prescribed surface fluxes exhibit near-surface temperatures that are systematically too cold compared to observations. This behavior reflects a fundamental limitation of prescribed-flux configurations: by imposing surface energy fluxes externally, the model atmosphere is prevented from dynamically adjusting surface fluxes in response to evolving near-surface stability, cloud cover, and radiative cooling. As a result, excessive nocturnal radiative cooling cannot be compensated by enhanced turbulent heat exchange from the surface, leading to unrealistically cold near-surface temperatures. This highlights that prescribed-flux simulations may mask physically relevant land–atmosphere feedbacks and should be interpreted cautiously when evaluating near-surface thermodynamic biases.

In terms of precipitation, the DP-SCREAM configuration with interactive land coupling more faithfully reproduces the well-documented global SCREAM bias of generating precipitation that is overly “bursty" and excessively intense (Tian et al., 2024; Bogenschutz et al., 2025b), whereas the configuration using prescribed surface fluxes exhibits a smoother and more gradual diurnal evolution that is closer to observations. Both DP-SCREAM configurations, however, produce precipitation peaks that occur too early in the afternoon, consistent with behavior seen in the global model (Donahue et al., 2024). In contrast, E3SM SCM does not exhibit a pronounced diurnal cycle of precipitation for either surface-flux configuration, a result also noted in earlier ~~SCM simulations with E3SMv1~~E3SMv1 SCM simulations (Bogenschutz et al., 2020). While the improved diurnal structure in DP-SCREAM may reflect advantages associated with explicitly resolving deep convection rather than parameterizing it, isolating this effect is challenging because SCREAM and E3SM SCM employ substantially different physical parameterizations, including turbulence, microphysics, and cloud–radiative interactions (Bogenschutz et al., 2025b).

An examination of the surface energy fluxes provides additional insight into the origin of these temperature and precipitation differences (Fig. 2). In DP-SCREAM simulations with interactive land coupling, latent heat fluxes are generally well represented, while sensible heat fluxes are systematically overestimated, particularly during the dry season. From an atmospheric modeling perspective, several mechanisms may contribute to this bias: overly efficient turbulent mixing in the boundary layer, excessive near-surface temperature gradients driven by warm atmospheric biases, or an exaggerated surface response to radiative forcing beneath deep convective anvils. The latter is consistent with previous findings that SCREAM exhibits an overac-

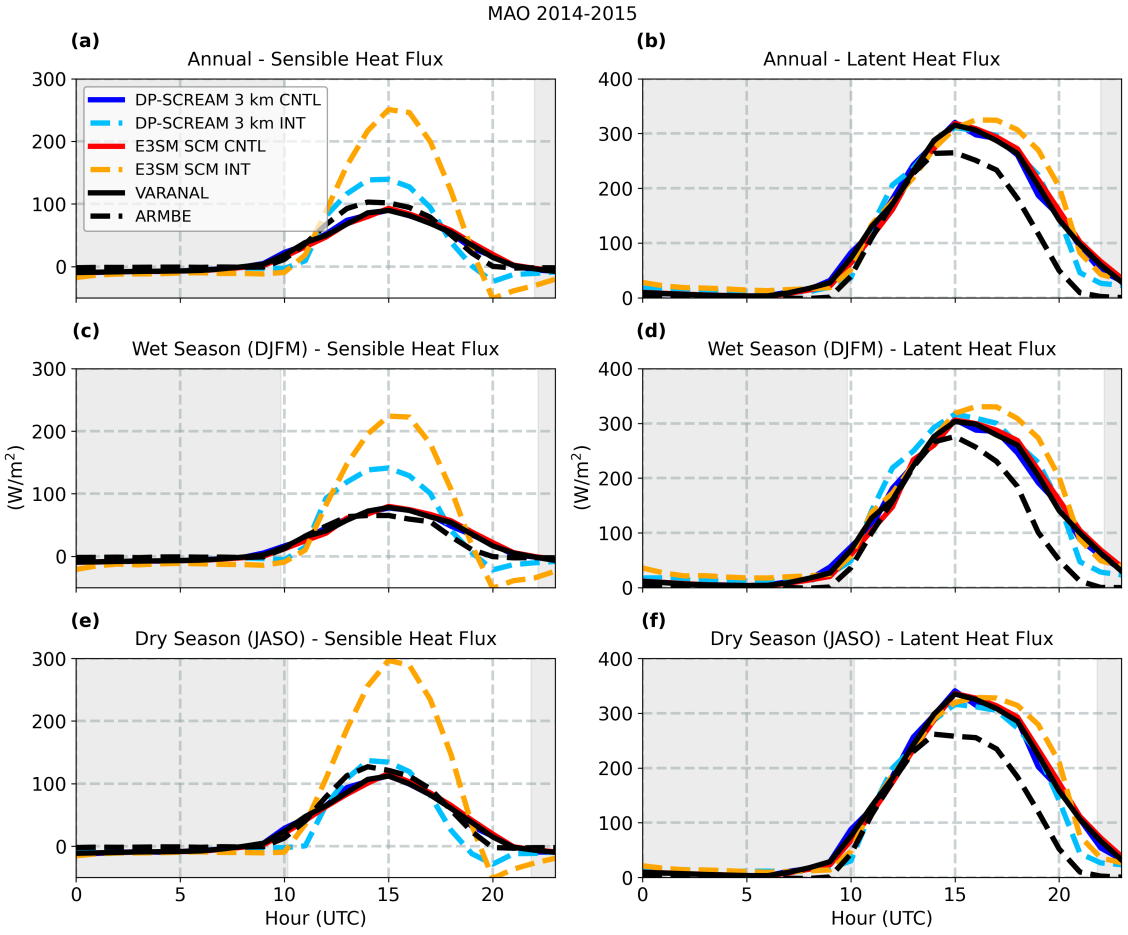

Figure 2. ~~Same as fig. 1 but for (left)~~ Diurnal composites of surface sensible heat flux ~~and~~ (~~right~~left column) and latent heat flux (right column) at GoAmazon for 2014–2015. Rows show annual, wet-season (December–March), and dry-season (July–October) composites, respectively. ARMBE observations are compared with E3SM SCM and DP-SCREAM at 3-km resolution. Solid model curves denote prescribed surface fluxes and dashed model curves denote interactive land; shading indicates nighttime, as in Fig. 1.

tive sensitivity of sensible heat flux to reductions in surface shortwave radiation during convective events (Tian et al., 2024). Notably, E3SM SCM exhibits an even larger sensible heat flux bias than SCREAM, suggesting that the error cannot be at-
290 tributed solely to convection-permitting dynamics. Instead, these results point to deficiencies in land–atmosphere coupling and boundary-layer physics that influence how surface energy imbalances are partitioned between sensible and latent heat fluxes. The resulting excess sensible heat flux in SCREAM likely reinforces its warm near-surface temperature bias, highlighting the need for targeted evaluation of land-surface coupling and nighttime boundary-layer mixing in these convection-permitting configurations.

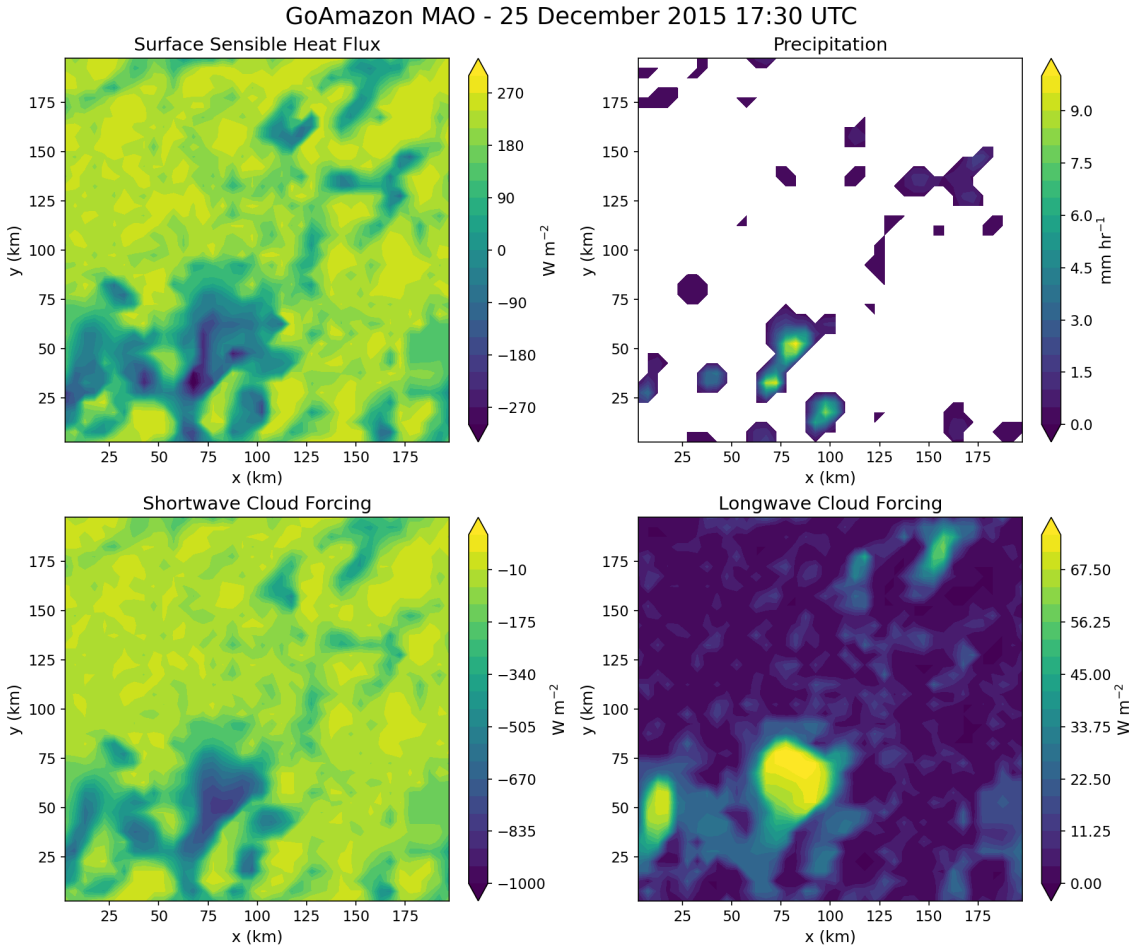

Figure 3. Snapshots of (top left) surface sensible heat flux, (top right) precipitation rate, (bottom left) shortwave cloud forcing, and (bottom right) longwave cloud forcing from DP-SCREAM 3 km simulation with interactive surface fluxes on 25 December 2015 at 17:30 UTC. Each panel shows the horizontal distribution across the doubly periodic domain at the same instant; colors indicate the variable and units identified by the corresponding color bar.

Figure 3 shows snapshots of the surface fluxes, precipitation, and cloud forcing from a strong convective event on 25 Decemeber 2015. This figure complements the analysis of Tian et al. (2024), who documented unrealistically large negative daytime sensible heat fluxes in global SCREAMv0 during deep convection. Their study demonstrated that SCREAM's land model can respond too strongly to reductions in surface shortwave radiation beneath optically thick anvils, producing extremely negative sensible heat fluxes (–100 to –300 W m^{-2}) over areas much larger than the precipitating convective cores. This overresponsiveness steepens the relationship between downward shortwave radiation and sensible heat flux, alters boundary-layer stability, and suppresses convective organization. Our long-term DP-SCREAM simulations reveal that analogous behavior occurs in the doubly periodic framework: over the two-year GoAmazon period, 68 percent of simulated DP-SCREAM days

exhibit occurrences of sensible heat fluxes below –300 W m^{-2}, indicating that the mesoscale land–atmosphere coupling issues identified by Tian et al. (2024) persist in the process-level modeling framework and can be readily reproduced and diagnosed within the DP configuration.

Additional insights emerge from the cloud and boundary-layer structure (Fig. 4). Annual diurnal composites show that both DP-SCREAM simulations capture the observed timing of the transition from shallow to deep convection; however, the interactive-land simulation produces more low-level boundary-layer cloud around 15 UTC, improving agreement with ARMBE, although shallow cloud cover remains underestimated. Conversely, the prescribed-flux simulation develops a persistent near-surface fog layer between 02 and 12 UTC. While fog is a naturally occurring feature of the Amazon during the wet season and can exert an important influence on the surface energy balance (Anber et al., 2015), the fog produced by the prescribed-flux simulation is substantially more persistent and extensive than indicated by ARMBE observations at the GoAmazon site. A similar fog bias was documented by Oware et al. (2025), who eliminated it by increasing SHOC's mixing length, suggesting that this spurious fog layer may be linked to overly strong nocturnal mixing combined with overly cool nighttime surface temperatures in the prescribed-flux configuration. In DP-SCREAM, the interactive-land mode suppresses this fog bias, likely because the warm nighttime temperature bias counteracts excessive near-surface saturation. In contrast, E3SM SCM does not exhibit a comparably strong fog bias but shows a generally weaker representation of the low-cloud diurnal cycle. The surface fog bias associated with prescribed surface flux simulations is discussed in greater detail in the context of the SGP results.

5.1.2 Southern Great Plains

Figure 5 shows seasonal diurnal composites of precipitation and 2-m air temperature derived from ten years of hindcast simulations at the ARM Southern Great Plains (SGP) site. In contrast to the GoAmazon site, where precipitation exhibits a pronounced diurnal cycle driven primarily by locally forced convection, precipitation at SGP is strongly influenced by large-scale synoptic forcing. This behavior is particularly evident during winter (DJF), the season with the lowest precipitation at SGP. During DJF, all model configurations exhibit broadly similar precipitation timing and amplitude, indicating that both E3SM SCM and DP-SCREAM similarly respond to large-scale forcing. However, all configurations show biases in precipitation magnitude relative to ARMBE observations, suggesting that simulated wintertime precipitation associated with synoptically forced systems may warrant further investigation. In particular, future work could examine whether these biases arise from excessive precipitation intensity during individual events or from an overly frequent occurrence of precipitation associated with frontal and stratiform systems.

During summer (JJA), precipitation at SGP displays a more complex structure, characterized by a late-afternoon~~peak~~ /early-evening peak at 02 UTC (approximately 20:00 local standard time; Fig. 5) associated with locally forced convection and a secondary nocturnal maximum linked to mesoscale convective systems propagating eastward across the central United States following convective initiation over the Rocky Mountains. The large-scale forcing provided to the process-level configurations contains sufficient information to capture this propagating convection, and all model configurations reproduce the timing and onset of the nocturnal precipitation maximum reasonably well. Among them, the E3SM SCM exhibits the clos-

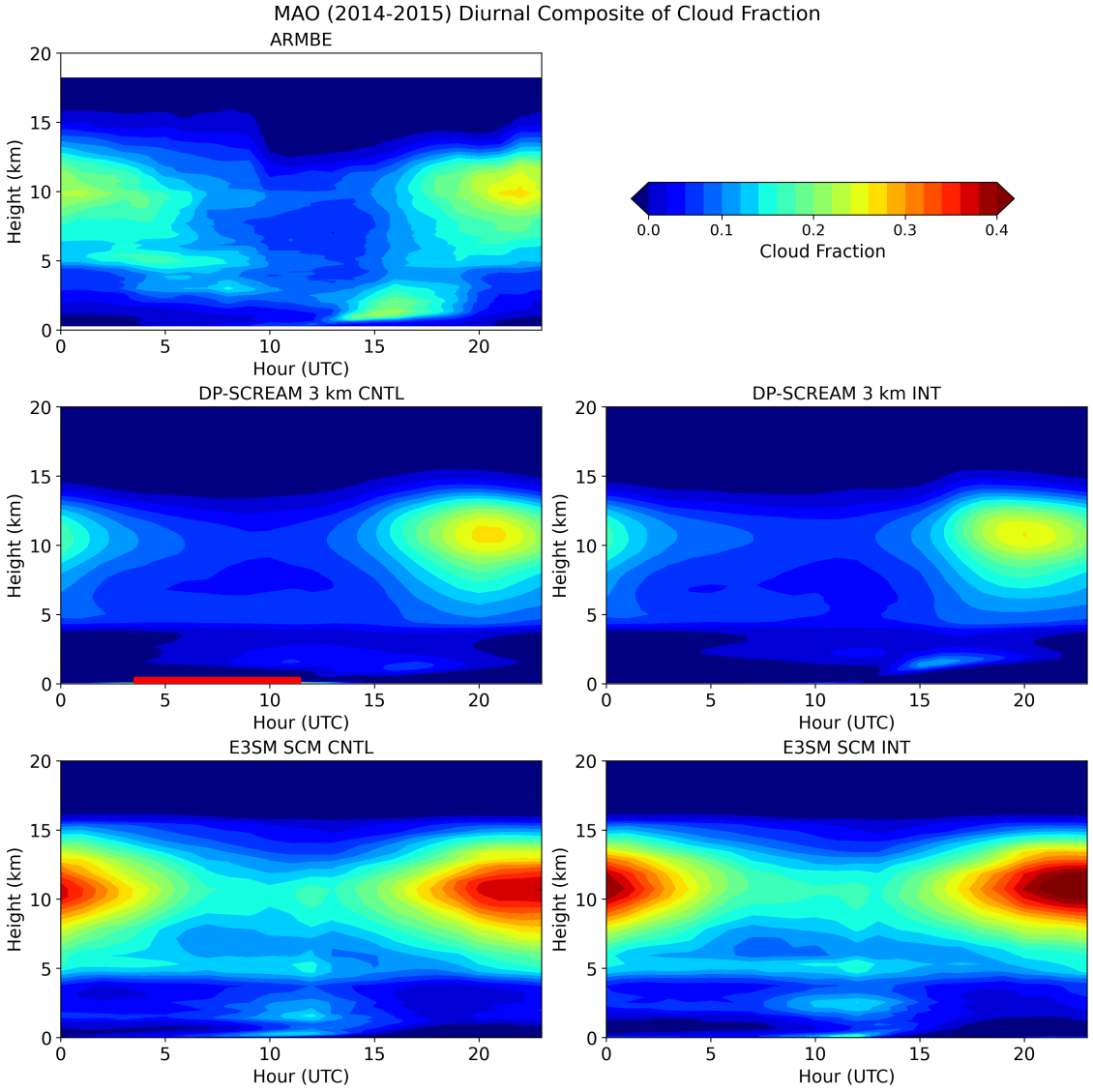

Figure 4. Annual diurnal ~~cycle~~ composites of cloud fraction ~~from (~~at GoAmazon for 2014–2015, shown as a function of UTC hour and height. The top row ~~)~~ shows ARMBE ~~, (~~observations; the middle ~~row) DP-SCREAM 3 km,~~ and ~~(~~bottom ~~row)~~ rows show DP-SCREAM at 3-km resolution and E3SM SCM, respectively. ~~To better highlight the~~ The left model column uses prescribed surface ~~fog bias,~~ fluxes (CNTL) and the ~~red line indicates periods~~ right model column uses interactive land (INT). Colors indicate cloud fraction. Red horizontal segments near the bottom of model panels mark hours when the mean cloud fraction at the lowest model level exceeds 0.3, highlighting the near-surface fog signal; they do not indicate cloud-layer depth.

est agreement with observed precipitation magnitude. In contrast, all configurations struggle to represent ~~the locally forced afternoon~~ this locally forced convection, which appears in ARMBE as a peak near 02 UTC. The E3SM SCM simulations

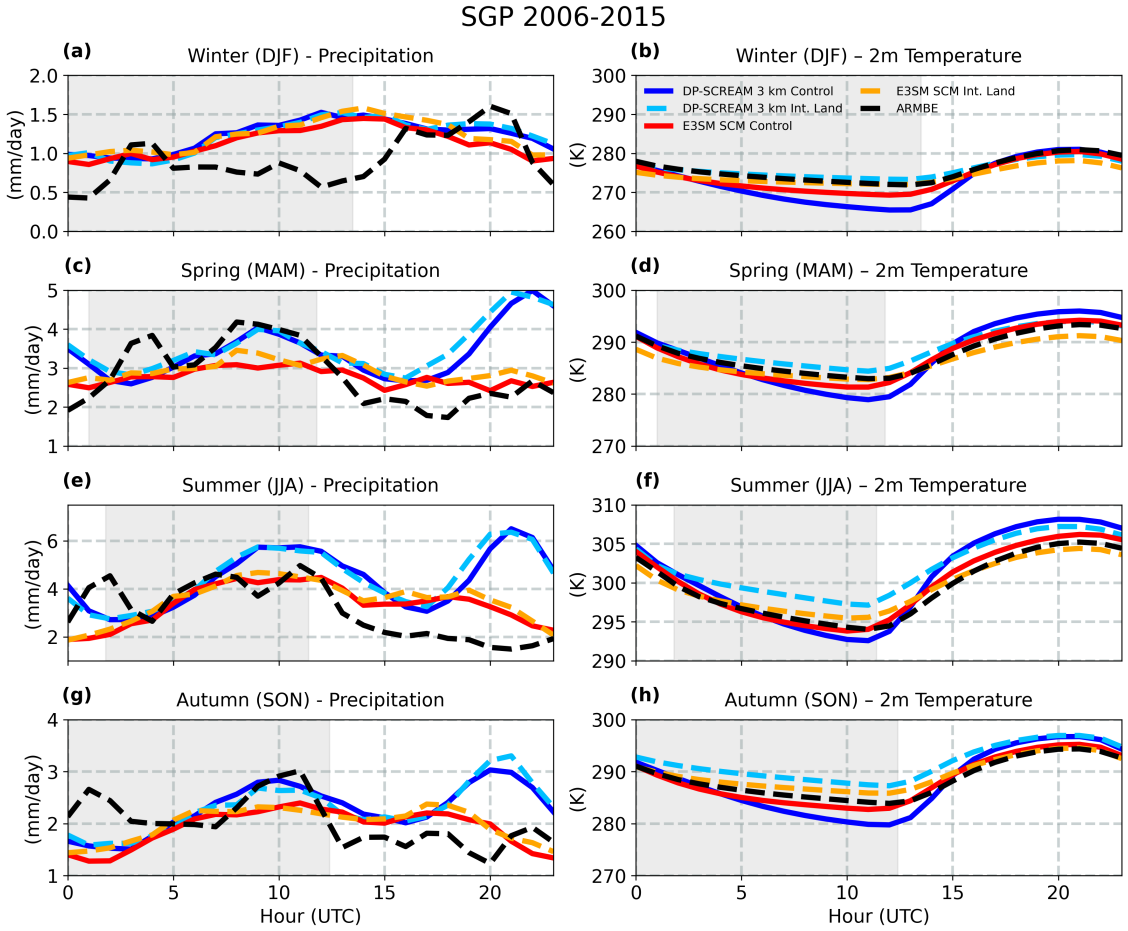

Figure 5. ~~Same as fig. 1 but for~~ Seasonal diurnal composites of precipitation rate (left column) and 2-m air temperature (right column) at the ARM Southern Great Plains site ~~and~~ for 2006–2015. Rows show winter (~~top row~~December–February)~~December – February~~, spring (~~second row~~March–May)~~March – May~~, summer (~~third row~~June–August)~~June – August~~, and autumn (~~bottom row~~September–November)~~September – November~~, respectively. ARMBE observations are compared with E3SM SCM and DP-SCREAM at 3-km resolution. Solid model curves denote prescribed surface fluxes and dashed model curves denote interactive land. Time is UTC and shading indicates nighttime.

largely miss this feature, while the SCREAM configurations produce precipitation that is both too early and too intense. This phasing bias is consistent with behavior seen in a range of global climate models, including both conventionally parameterized and storm-resolving systems. Notably, precipitation at SGP shows relatively little sensitivity to whether surface fluxes are prescribed or interactively coupled, in contrast to results at the GoAmazon site.

In contrast to precipitation, the diurnal composites of 2-m temperature reveal a strong dependence on surface-flux treatment. For all seasons, simulations employing prescribed surface fluxes exhibit a pronounced negative nighttime temperature bias, a behavior not present in global SCREAM simulations (Donahue et al., 2024). Configurations with interactive land coupling more

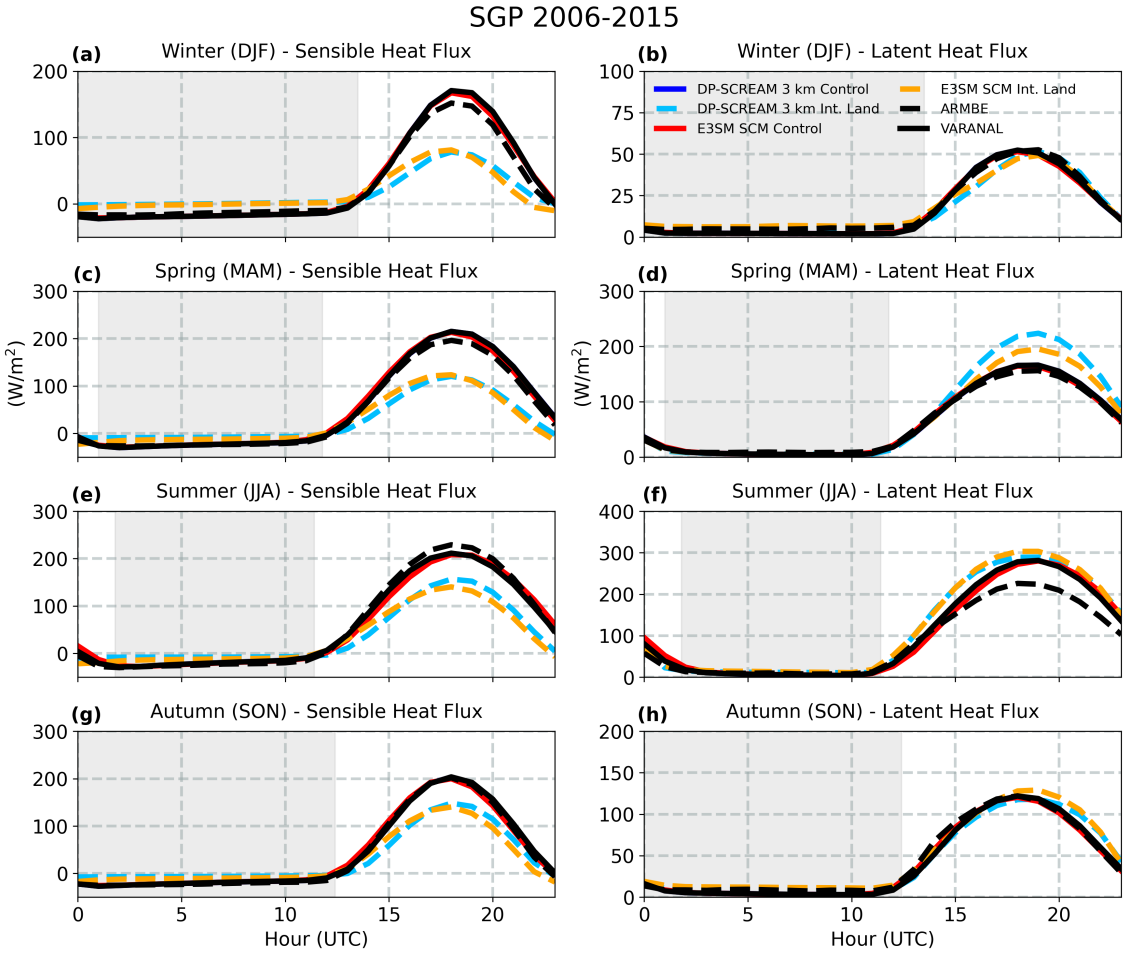

Figure 6. ~~Same as fig. 5 but for~~ Seasonal diurnal composites of surface sensible heat flux (left column) ~~sensible~~ and latent heat flux ~~and~~ (right column) ~~latent heat flux)~~at the ARM Southern Great Plains site for 2006–2015. Rows show winter, spring, summer, and autumn, respectively. ARMBE observations are compared with E3SM SCM and DP-SCREAM at 3-km resolution. Solid model curves denote prescribed surface fluxes and dashed model curves denote interactive land. Time is UTC and shading indicates nighttime.

closely reproduce the temperature biases seen in global simulations, characterized by warm biases during both nighttime and daytime hours. These temperature biases are most pronounced during summer and are larger in SCREAM than in E3SM SCM, consistent with results from the GoAmazon site. This behavior suggests that both land–atmosphere coupling and SCREAM's boundary-layer parameterization, particularly under stable nighttime conditions, play important roles in shaping near-surface
350 temperature biases. Nevertheless, both SCREAM and E3SM SCM perform relatively well during winter and spring, indicating that warm-season processes are likely the dominant contributors to continental midlatitude temperature biases in these models.

Figure 6 presents diurnal composites of sensible and latent heat fluxes at the SGP site. Consistent with results from the GoAmazon analysis, both E3SM SCM and SCREAM reasonably capture the magnitude and phasing of latent heat fluxes

across seasons, although a systematic overestimation is evident during spring. In contrast, substantially larger differences emerge in the sensible heat flux. During nighttime hours, both model configurations exhibit a positive sensible heat flux bias, ~~likely associated with excessive boundary-layer mixing that maintains overly~~ whereas a negative bias occurs during daylight hours. These flux biases coexist with warm near-surface ~~temperatures. This warm nighttime bias subsequently contributes to an overly stabilized surface layer during the daytime, leading to a compensating negative bias in sensible heat flux during daylight hours~~air temperature biases in the interactive-land simulations, but the diurnal composites alone do not establish their underlying mechanisms or a causal connection between the nighttime and daytime errors. Attribution of these biases requires further analysis of surface–air temperature differences, atmospheric temperature profiles, turbulent heat transport, and the surface energy budget. The daytime sensible heat flux deficit is accompanied by an overestimation of latent heat flux, particularly during spring, suggesting that excessive precipitation may lead to overly wet soils and a partitioning of available surface energy toward evaporation rather than sensible heating. Unlike the GoAmazon site, where soil moisture remains abundant for much of the year and evapotranspiration is primarily energy limited, the semi-arid grassland and cropland environment at SGP is more strongly influenced by soil moisture availability. Consequently, precipitation biases can have a larger impact on land-atmosphere coupling and the partitioning of surface turbulent fluxes at SGP than at the Amazon site.

Following the analysis performed for the GoAmazon site, we also examined the occurrence of extreme negative sensible heat flux events in DP-SCREAM, defined here as values less than –300 W m^{-2}. At SGP, such events occur far less frequently than over the Amazon, appearing in only approximately 7% of simulated days. This reduced frequency is consistent with the weaker coupling between deep convection, cloud radiative effects, and land–atmosphere feedbacks at midlatitude continental sites compared to tropical environments. Differences in soil moisture regime may also contribute to this behavior. At the Amazon site, soils remain relatively moist throughout much of the year, and evapotranspiration is often energy limited. Consequently, reductions in surface net radiation associated with deep convective cloud systems are expressed primarily through decreases in sensible heat flux, promoting the occurrence of strongly negative values. In contrast, at SGP, where evapotranspiration is more strongly influenced by soil moisture availability, changes in net radiation can be partitioned between both sensible and latent heat fluxes. This additional degree of freedom reduces the tendency for large reductions in sensible heat flux and may partially explain the lower frequency of extreme negative events.

Diurnal composites of cloud fraction for observations and each model configuration, stratified by season, are shown in Figure 7. Several notable features emerge from these composites. Most prominently, clear differences are evident between simulations using prescribed surface fluxes and those employing interactive land coupling, for both E3SM SCM and SCREAM. In configurations with prescribed surface fluxes, a persistent nighttime fog layer develops near the surface across all seasons. This feature is absent in the corresponding global simulations but has been documented previously in DP-SCREAM and E3SM SCM experiments using prescribed surface fluxes (Oware et al., 2025). In contrast, simulations with interactive surface fluxes do not exhibit this fog layer.

The presence of the fog layer in the prescribed-flux simulations is closely tied to a cold near-surface temperature bias, which promotes excessive nighttime saturation and low-level cloud formation. When interactive land–atmosphere coupling is enabled, both E3SM SCM and SCREAM instead exhibit a warm near-surface temperature bias that suppresses saturation and effectively

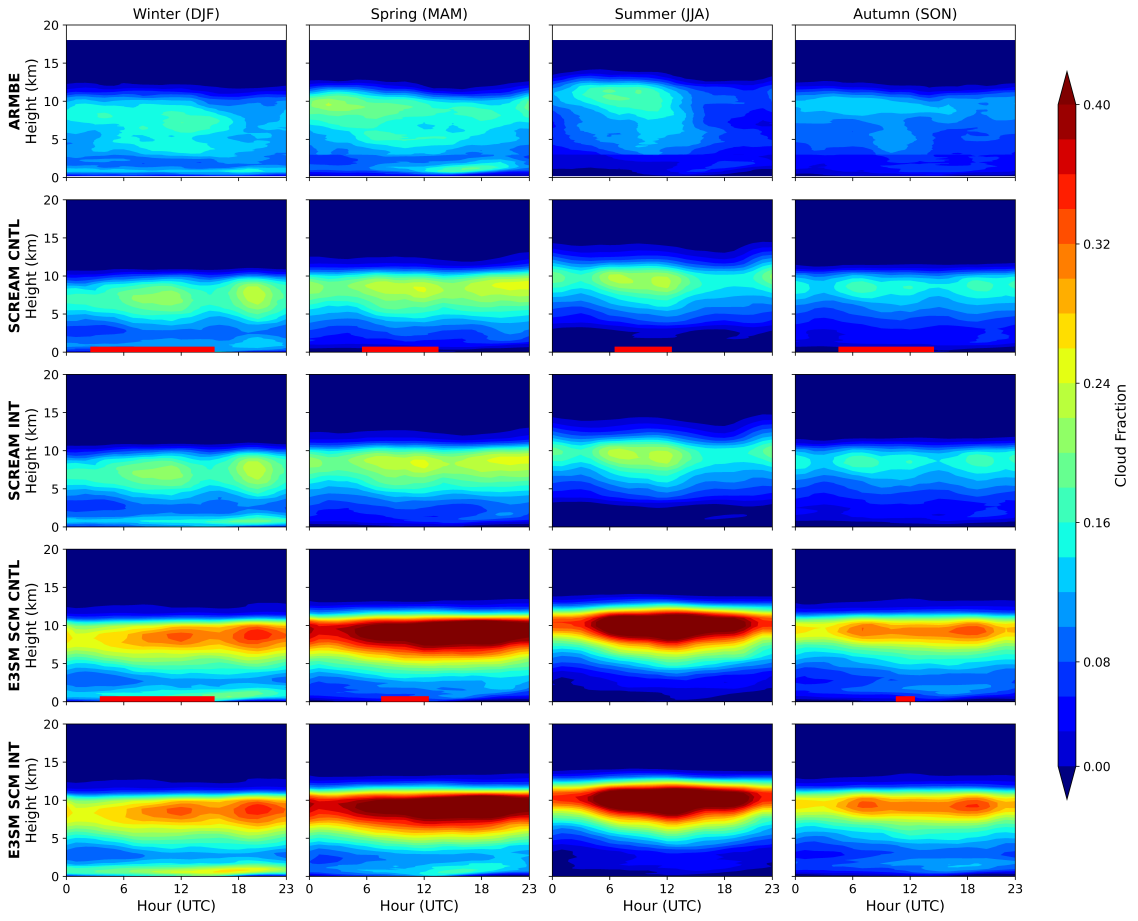

Figure 7. ~~Diurnal cycle~~ Seasonal diurnal composites of cloud fraction at the ARM Southern Great Plains site for ~~(top row)~~ 2006–2015, shown as a function of UTC hour and height. Rows show ARMBE observations, ~~(second row)~~ DP-SCREAM ~~3 km control~~ at 3-km resolution with prescribed surface fluxes ~~,~~ (~~third row~~CNTL), DP-SCREAM ~~3 km~~ with interactive ~~surface fluxes,~~ land (~~fourth row~~INT), E3SM SCM with prescribed surface fluxes, and ~~(bottom row)~~ E3SM SCM with interactive ~~surface fluxes for~~ land, respectively. Columns show winter (~~first column~~December–February)~~winter~~, spring (~~second column~~March–May)~~spring~~, summer (~~third column~~June–August)~~summer~~, and autumn (~~fourth column~~September–November)~~autumn~~. ~~To better highlight~~ Colors indicate cloud fraction. Red horizontal segments near the ~~surface fog bias, the red line indicates periods~~ bottom of model panels mark hours when the mean cloud fraction at the lowest model level exceeds 0.3. These segments highlight the near-surface fog signal, which is difficult to distinguish on the full-height color scale, and do not indicate cloud-layer depth.

eliminates the fog layer. This behavior highlights the strong sensitivity of nocturnal boundary-layer cloudiness to surface en-
390 ergy exchange and underscores the importance of interactive land coupling for faithfully representing nighttime thermodynamic

structure. The appearance of a negative temperature bias in simulations with prescribed surface fluxes indicates that this configuration artificially decouples the atmosphere from surface energy constraints, preventing compensating land–atmosphere feedbacks that would otherwise moderate nocturnal cooling. In other words, the prescribed-flux setup imposes surface conditions that are thermodynamically inconsistent with the evolving atmospheric state, leading to unrealistically strong nighttime cooling, excessive saturation, and spurious fog formation. This suggests that the fog layer is not a robust physical response of the atmospheric model itself, but rather an artifact of the prescribed surface-flux configuration.

Overall, simulations employing interactive surface fluxes exhibit closer agreement with ARMBE observations than those using prescribed fluxes. During winter, the persistent low-level stratiform cloud layer observed at SGP is more accurately represented when land–atmosphere coupling is enabled. In spring, ARMBE reveals a pronounced signal of locally forced shallow cumulus developing during the afternoon. This feature is captured remarkably well by the E3SM SCM with interactive surface fluxes, whereas DP-SCREAM produces only a weak signature and fails to represent it altogether when prescribed surface fluxes are used. One plausible explanation is that the spurious low-level fog layer present in the prescribed-flux simulations suppresses the development of locally forced shallow convection by altering near-surface thermodynamic structure. The reason that DP-SCREAM represents the observed shallow cumulus less accurately than the E3SM SCM even when both use interactive land remains unresolved and warrants targeted investigation in future work.

In contrast, high-level cloud occurrence exhibits a different behavior. E3SM SCM systematically overestimates high-level cloud fraction, while SCREAM shows closer agreement with ARMBE. Notably, the simulation of high-level clouds appears relatively insensitive to whether surface fluxes are prescribed or interactively coupled, suggesting that land–atmosphere coupling primarily influences low-level cloud processes at SGP.

5.2 Process-Level Cases

Previous work demonstrated that DP-SCREAM at 3-km resolution, as well as higher-resolution configurations, exposes distinct process-level biases associated with the model physics (Bogenschutz et al., 2025b). For continental cases, the CASS simulation reproduced a persistent bias in which shallow convection failed to deepen sufficiently at 3-km resolution. In the GoAmazon single- and double-pulse cases, DP-SCREAM at 3 km exhibited an intense, short-lived burst of precipitation followed by suppressed convection. Moreover, both the 3-km and higher-resolution configurations failed to organize convection and exhibited a deficit of mid-level congestus, biases that closely resemble those seen in the global model. Based on these similarities, the previous study concluded that these short process-level cases provide efficient proxies for diagnosing and understanding large-scale model biases. However, those simulations employed prescribed surface fluxes. In this section, we investigate the impact of including an interactive land model in these process-level cases to assess the role of land–atmosphere coupling in shaping these biases. Specifically, we examine whether interactive coupling mitigates or alters the previously identified errors and whether neglecting land–atmosphere interactions limits the utility of these cases as faithful proxies for reproducing model behavior. These results provide guidance for future users seeking to employ these cases to diagnose and replicate process-level biases.

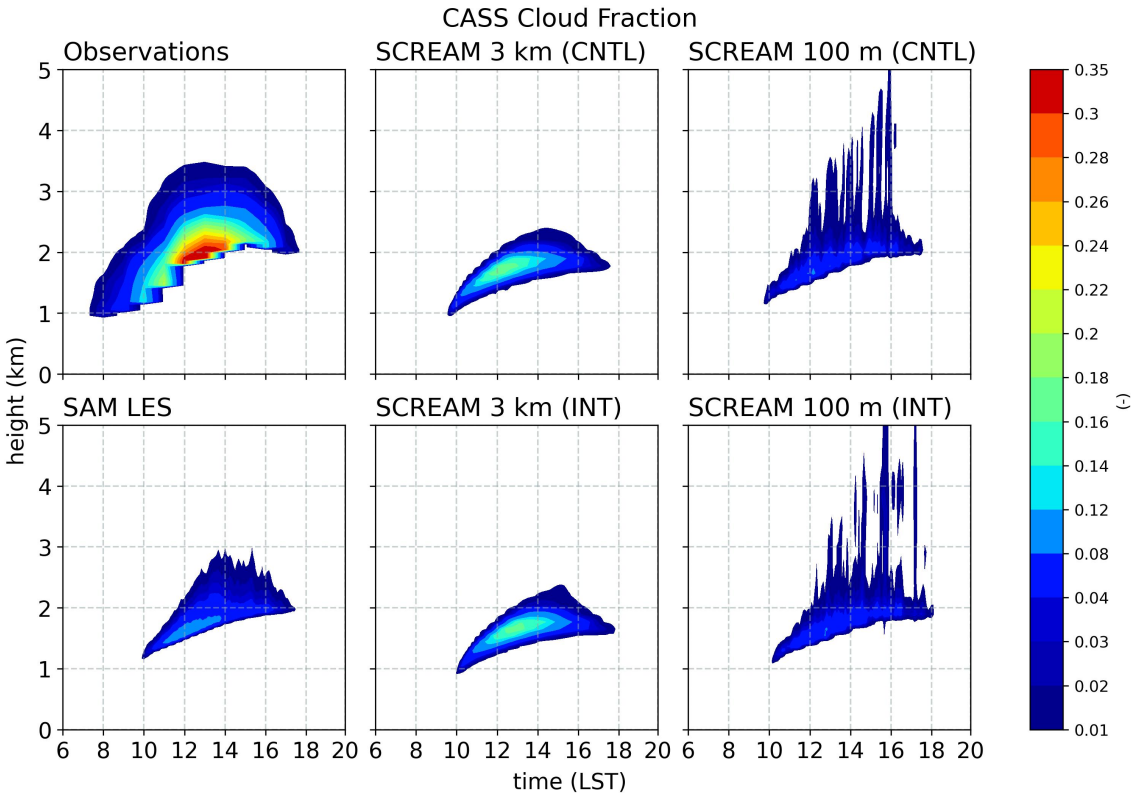

Figure 8. ~~Evolution~~ Time–height evolution of cloud fraction for the CASS continental shallow-cumulus case. ~~For~~ The left column shows observations (top) and SAM LES ~~and SCREAM simulations the panels represent the horizontally averaged cloud fraction. Observational reference is Active Remote Sensing of Clouds (ASRCL~~bottom~~). For~~ ; the middle and right columns show DP-SCREAM at 3-km and 100-m resolution, ~~simulations with (~~respectively. DP-SCREAM panels in the top row ~~)~~ use prescribed surface fluxes ~~and~~ (CNTL), while those in the bottom row ~~)~~ use interactive ~~surface fluxes~~ land (INT). Model cloud fractions are ~~shown~~horizontal domain averages. Colors indicate cloud fraction and time is local standard time (LST). Observations are from the Active Remote Sensing of Clouds product.

In this section we ~~only consider results for~~ compare DP-SCREAM ~~. For our large eddy simulation (LES) reference, we use the System for Atmospheric Modeling (SAM; Khairoutdinov and Randall, 2003). The horizontal and vertical resolutions, domain size, and time steps for the SAM simulations discussed in this paper vary by case. Detailed descriptions can be found in Bogenschutz et al. (2025b)~~results with the SAM LES references introduced in Section 2.1; their configurations are summarized in Table 1.

5.2.1 CASS - Continental Shallow Convection

Figure 8 shows the temporal evolution of cloud fraction for observations, SAM-LES, DP-SCREAM at 3-km resolution, and DP-SCREAM at 100-m resolution. For the DP-SCREAM simulations, both the control configuration with prescribed surface fluxes

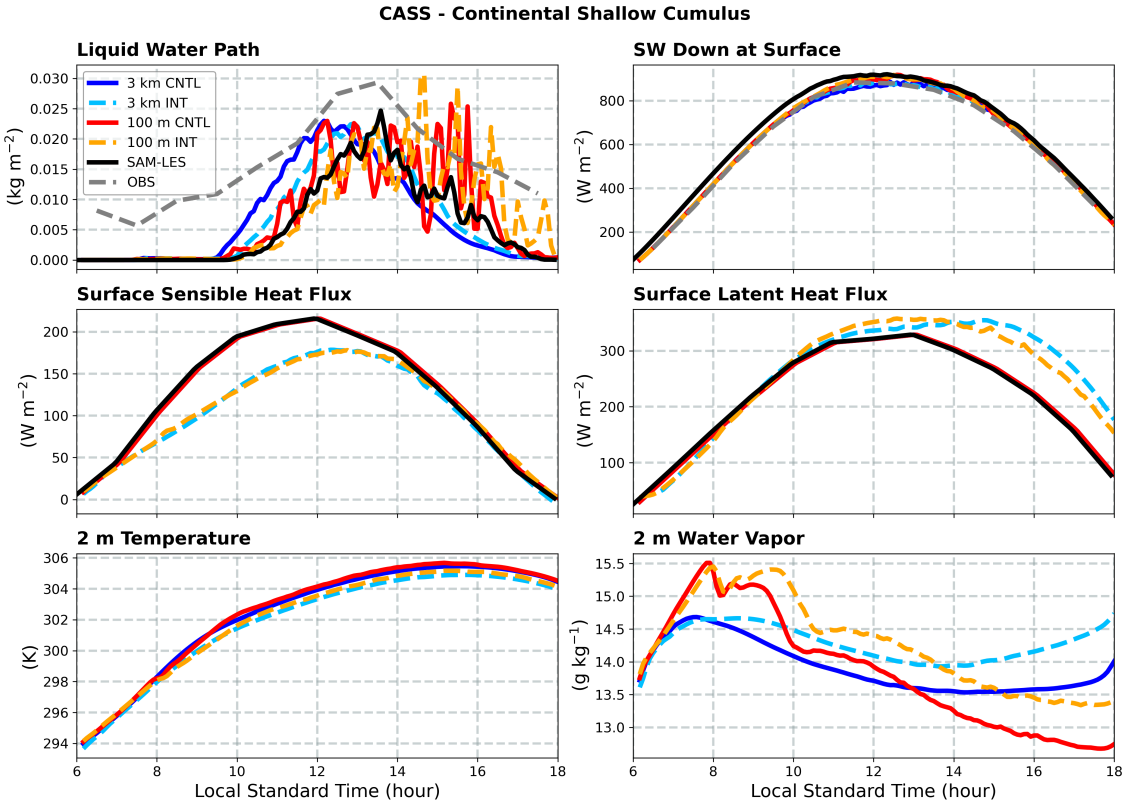

Figure 9. Temporal evolution of the (top left) liquid water path, (top right) Shortwave downwelling at the surface, (middle left) surface sensible heat flux, (middle right) surface latent heat flux, (bottom left) 2 m near surface Temperature, and (bottom right) near surface water vapor for the CASS case. Model curves compare DP-SCREAM at 3-km and 100-m resolution with prescribed surface fluxes (solid) and interactive land (dashed), alongside SAM LES and observations where available. DP-SCREAM and SAM quantities are horizontal domain averages. Time is local standard time.

and the configuration with interactive land coupling are presented. Across both resolutions, the inclusion of land–atmosphere coupling has minimal impact on the overall evolution of cloud fraction.

Consistent with Bogenschutz et al. (2025b), the 3-km simulations produce clouds that are systematically too shallow, a bias that persists when interactive land coupling is enabled. Increasing resolution to 100 m improves the representation of cloud depth, likely due to reduced dependence on subgrid-scale parameterizations, but does so at the expense of cloud amount, and the simulated clouds become too deep relative to observations. Importantly, these structural biases in cloud depth and organization are largely unchanged by the inclusion of interactive land–atmosphere coupling. This insensitivity suggests that the dominant errors arise from intrinsic aspects of the model physics and/or dynamics rather than from errors in land–atmosphere interactions.

These findings are further reflected in Fig. 9, which presents the temporal evolution of liquid water path alongside several surface-related variables. Although the 3-km simulation with interactive land coupling exhibits a slightly delayed onset of

cloud development relative to the control configuration with prescribed surface fluxes, the overall cloud evolution remains nearly identical between the two simulations. The interactive configurations show modestly higher 2-m water vapor and slightly warmer 2-m air temperatures compared to the prescribed-flux simulations. These differences are consistent with changes in the surface energy balance: interactive simulations exhibit reduced sensible heat fluxes and somewhat enhanced latent heat fluxes relative to the prescribed values, leading to increased near-surface moisture and a redistribution of surface heating toward evaporative cooling. Despite these thermodynamic adjustments near the surface, the large-scale cloud evolution and associated liquid water path biases remain largely unchanged. This insensitivity indicates that the persistent cloud biases in this case are not contingent on whether surface fluxes are prescribed or interactively computed.

5.2.2 GoAmazon - Shallow to Deep Convective Transition

Figures 10 and 11 show the evolution of cloud fraction and precipitation rate, respectively, along with key near-surface thermodynamic and surface flux variables for the GoAmazon single- and double-pulse transition cases. Consistent with the CASS results, the inclusion of interactive land–atmosphere coupling has little influence on the overall evolution of these process-level simulations. For both the single- and double-pulse cases, the 3-km DP-SCREAM simulations produce precipitation that is overly intense and excessively "bursty," regardless of whether surface fluxes are prescribed or interactively computed. While subtle differences in precipitation onset timing and peak intensity are evident between the two surface configurations, the overall character and magnitude of the simulated convective response remain nearly identical. At 250-m resolution, the DP-SCREAM simulations show even less sensitivity to the choice of surface flux treatment. As reported in Bogenschutz et al. (2025b), the 250-m configuration reasonably reproduces the observed and LES precipitation evolution for the single-pulse case but fails to capture the second precipitation pulse in the double-pulse case.

The limited sensitivity to surface flux treatment is consistent with the CASS analysis, which showed that interactive land primarily alters the partitioning of surface energy between sensible and latent heat fluxes. These changes can influence boundary-layer growth and cloud-base height, thereby affecting the timing of convective initiation. However, once deep convection develops, the subsequent cloud evolution and precipitation characteristics remain largely unchanged. This behavior is particularly evident at the GoAmazon site, where abundant soil moisture limits the extent to which enhanced evaporation can modify the surface energy balance. The persistence of the double-pulse bias in both prescribed and interactive land configurations therefore suggests that it is unlikely to arise from deficiencies in land–atmosphere coupling. Instead, the bias appears to be associated with the representation of the shallow-to-deep convective transition itself. Specifically, the absence of a well-defined mid-level congestus phase, previously identified by Tian and Zhang (2025) as a critical precursor to the observed convective evolution, points toward deficiencies in the representation of cloud-top growth, entrainment processes, or the ability of cloudy updrafts to penetrate the cloud-top inversion. These results suggest that the dominant limitations reside in SCREAM's physical parameterizations, resolved dynamics, or their interaction rather than in the treatment of surface fluxes.

In terms of surface fluxes, both SCREAM configurations exhibit sensible heat fluxes that are too weak at initialization, likely reflecting inherited biases from the land model initial condition file. Following initialization, the simulated sensible and latent heat fluxes are reasonably well represented in the double-pulse case when compared to observations. In contrast, the single-

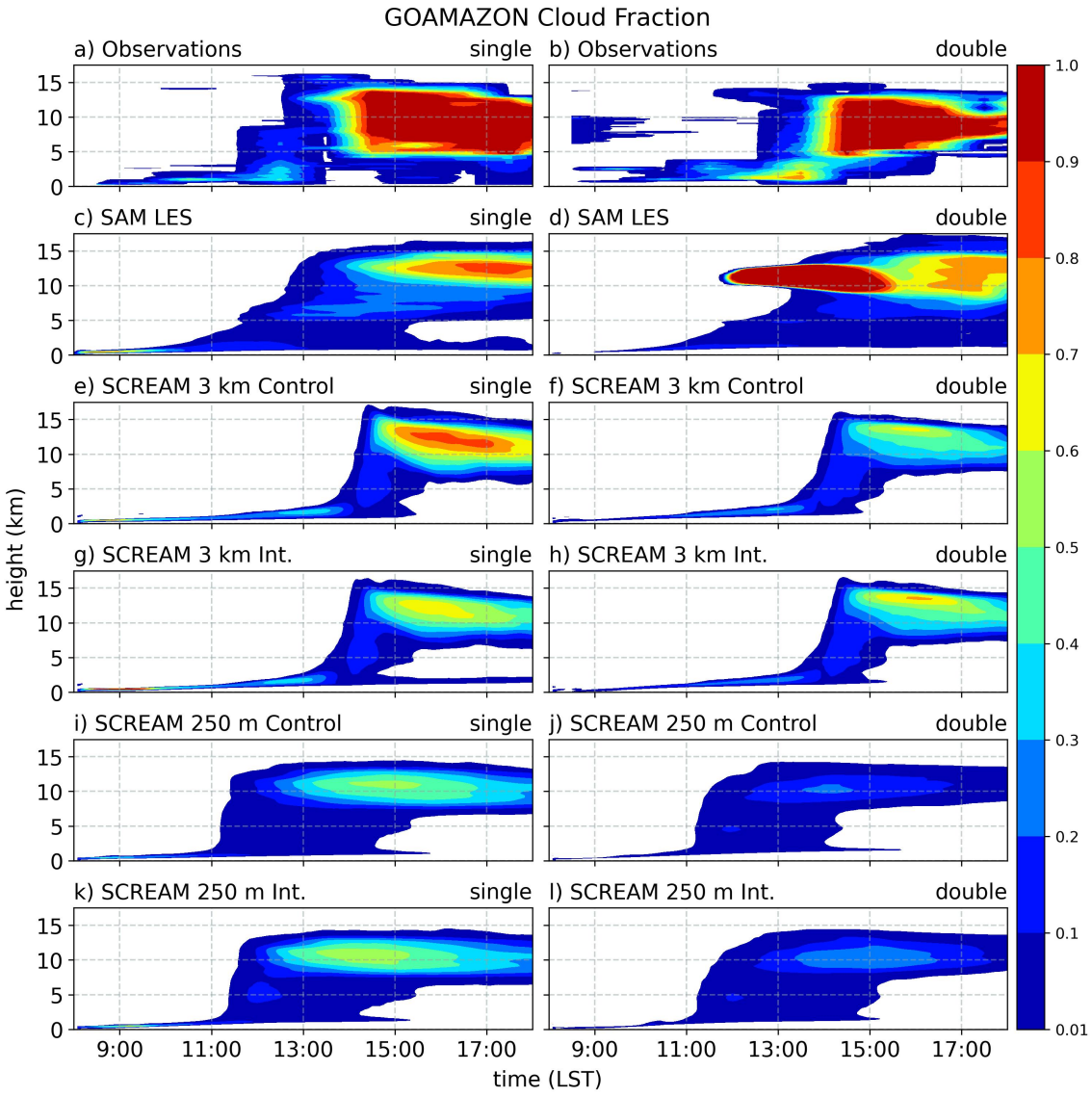

Figure 10. ~~Evolution~~ Time–height evolution of ~~the~~ cloud fraction for the ~~two days of the~~ GoAmazon single-pulse case ~~. The left column represents the "single pulse" day initialized~~ on ~~05~~ 5 October 2014 ~~while the right~~ (left column~~represents the "double pulse" day initialized~~) and double-pulse case on 26 August ~~2015. For~~ 2015 (right column). Rows show observations, SAM LES, DP-SCREAM at 3-km resolution with prescribed surface fluxes, DP-SCREAM at 3-km resolution with interactive land, DP-SCREAM at 250-m resolution with prescribed surface fluxes, and ~~SCREAM simulations all curves represent the~~ DP-SCREAM at 250-m resolution with interactive land, respectively. Model cloud fractions are horizontal domain averages. Colors indicate cloud fraction and time is local standard time (LST). Observations are from the Active Remote Sensing of Clouds ~~(ASRCL)~~product.

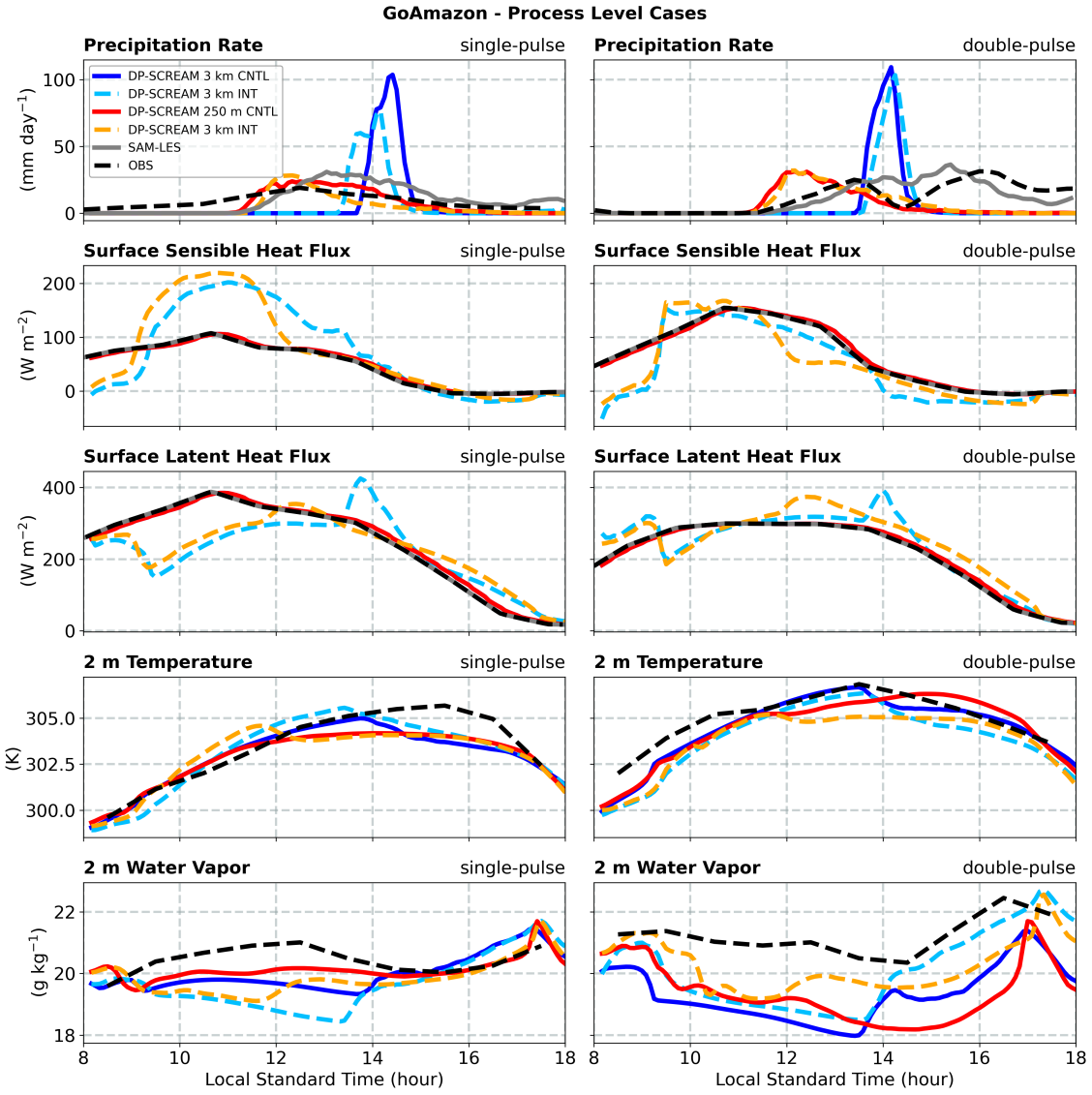

Figure 11. Evolution of the (top row) precipitation rate, (second row) surface sensible heat flux, (third row) surface latent heat flux, (fourth row) 2 m temperature, and (bottom row) 2 m water vapor for the (left column) single-pulse case and (right column) double-pulse case. DP-SCREAM curves compare 3-km and 250-m resolution with prescribed surface fluxes (solid) and interactive land (dashed); SAM LES and observations are included where available. Model quantities are horizontal domain averages and time is local standard time.

pulse case shows a substantial overestimate of sensible heat flux during the daytime, potentially linked to excessive incoming solar radiation and subsequent surface warming in the model. Despite these thermodynamic differences near the surface, the fundamental precipitation and cloud evolution biases remain largely unaffected by the inclusion of interactive land coupling, reinforcing the conclusion that land–atmosphere interactions are not the primary driver of the identified process-level errors.

6 Summary and Discussion

This study extends E3SM's process-level modeling capabilities by establishing a practical and scientifically consistent workflow for running both the E3SM ~~single-column model (SCM)~~ SCM and doubly periodic SCREAM (DP-SCREAM) with a fully interactive land surface. While the technical option for interactive land has existed, its broader use has been limited by the requirement for realistic, spun-up land initial conditions. We address this barrier by (i) generating a physically equilibrated land state from an offline-forced, multi-year E3SM/ELM simulation, (ii) selecting restart files consistent with the month and year of each observational campaign for long-term hindcasts, and (iii) developing an offline preprocessing approach that maps and replicates a representative ELM grid cell (including its landunit/column/PFT hierarchy) across the DP-SCREAM doubly periodic domain without modifying ELM's core PIO infrastructure. Combined with a two-day hindcast protocol initialized daily, retaining only day two for analysis, this workflow enables robust, reproducible, and computationally efficient long-term and short-term process-level simulations that remain closely constrained by observed large-scale forcing while still expressing intrinsic model biases.

Applying this framework to two years of GoAmazon hindcasts and ten years of SGP hindcasts demonstrates that interactive land coupling is essential for reproducing key near-surface thermodynamic biases characteristic of global simulations. At both sites, simulations employing prescribed surface fluxes develop systematically cold near-surface temperatures, especially at night, a behavior inconsistent with global SCREAM and indicative of thermodynamic inconsistency between imposed fluxes and the evolving atmospheric state. In contrast, interactive-land simulations reproduce the sign and diurnal structure of the warm near-surface bias seen in global SCREAM, including a systematic nocturnal warm bias in DP-SCREAM that is absent in E3SM SCM. These long-term results support the conclusion that the "too warm surface" bias over land is strongly tied to land–atmosphere coupling and its interaction with boundary-layer processes. At GoAmazon, interactive coupling also yields precipitation behavior more consistent with the known global SCREAM tendency toward overly intense, "bursty" precipitation, while prescribed-flux simulations appear artificially smoothed and closer to observations, highlighting that prescribed fluxes can mask coupled feedbacks relevant to global-model behavior.

The long-term simulations further show that interactive land coupling substantially improves the realism of nocturnal low-level cloudiness by avoiding the persistent near-surface fog layer that emerges in prescribed-flux runs, particularly at SGP. The evidence across both sites indicates that this fog bias is closely linked to the cold nighttime 2-m temperature bias in prescribed-flux configurations, which promotes excessive saturation and spurious low cloud formation. When interactive coupling is enabled, the surface energy budget can respond dynamically to evolving stability and radiative cooling, moderating nocturnal cooling and thereby suppressing unrealistically frequent near-surface saturation. This interpretation is consistent with earlier work showing sensitivity of the fog bias to boundary-layer mixing characteristics, and it underscores that the prescribed-flux configuration can generate artifacts that are not representative of either observations or the parent global model. Taken together, these results argue that long-term, land-based process-level hindcasts intended to diagnose climatological thermodynamic biases or boundary-layer cloud structure should preferentially employ interactive land coupling.

In contrast, the short process-level cases indicate that many cloud and convection "process" biases targeted by case-study frameworks are largely insensitive to whether surface fluxes are prescribed or interactively computed. For the continental shallow convection (CASS) case, DP-SCREAM at 3 km continues to produce clouds that are too shallow, and higher resolution reduces reliance on subgrid-scale closures but introduces compensating errors in cloud amount and/or cloud depth; these behaviors persist with interactive land coupling. For the GoAmazon single- and double-pulse transition cases, DP-SCREAM at 3 km produces precipitation that is overly intense and episodic under both surface treatments, and the high-resolution configuration reproduces the single-pulse precipitation evolution while still failing to capture the second pulse in the double-pulse case. The persistence of these errors with and without interactive coupling indicates that they arise primarily from deficiencies internal to the atmospheric model (such as physics, resolved dynamics, or their coupling) rather than from land–atmosphere feedbacks. Thus, while interactive land coupling can strongly influence long-term thermodynamic biases and nocturnal boundary-layer cloud artifacts, it does not appear to be the controlling factor for the targeted convection-organization and congestus-related deficiencies emphasized in these short case studies.

These findings have practical implications for community use of E3SM process-level configurations. When the goal is to replicate, understand, or attribute climatological near-surface temperature biases, boundary-layer thermodynamic structure, or low-cloud artifacts in long-term hindcasts over land, interactive land coupling should be considered the default choice because it permits the coupled feedbacks that are active in the parent global model. Prescribed surface flux simulations remain useful for tightly constrained sensitivity studies, but they can introduce thermodynamic inconsistencies and artifacts (e.g., spurious nighttime cooling and fog) that complicate interpretation of near-surface biases. Conversely, when the primary goal is to expose and diagnose intrinsic cloud and convection process-level biases, such as insufficient deepening of shallow convection, deficits of mid-level congestus, or failures of convective organization, the choice of prescribed versus interactive surface fluxes has little impact on the qualitative conclusions in the cases examined here. For these targeted process-level applications, either surface treatment may be used without materially altering the key bias signals, whereas long-term hindcast studies focused on coupled land–atmosphere biases should employ interactive fluxes to ensure fidelity to global-model behavior.

Beyond bias diagnosis, this capability provides a controlled framework for investigating local land–atmosphere feedbacks (Santanello et al., 2018). Coupling is expected to be particularly consequential during soil-moisture transitions between wet and dry conditions, when evapotranspiration and surface energy partitioning respond strongly to water availability, and during clear, weak-wind nights when surface cooling and turbulent exchange jointly govern near-surface stability. Sensitivity experiments perturbing initial soil moisture, prescribed vegetation properties, or land-surface parameters could quantify their effects on boundary-layer growth, entrainment, cloud-base height, and convective initiation. Paired experiments could also examine how cloud-induced changes in surface radiation modify turbulent fluxes and subsequent cloud development, and how soil heat storage and atmospheric mixing influence nocturnal cooling, dew or fog formation, and the morning transition. Comparing these responses between E3SM SCM and DP-SCREAM would help assess how parameterized versus explicitly represented convection interacts with land feedbacks, while recognizing that the models also differ in other physical parameterizations. These applications are prospective and were not systematically tested here. The present homogeneous land initialization and prescribed large-scale atmospheric forcing support studies of local feedbacks, whereas questions involving imposed

land-surface heterogeneity, regional circulation responses, or accumulated drought feedbacks would require additional experimental design, spatially varying land initialization, or longer continuous integrations.

Although this study focuses on continental cases, analogous questions arise for air–sea interactions. Oceanic cases in E3SM SCM and DP-SCREAM support either prescribed surface fluxes or fluxes calculated from the evolving atmospheric state and prescribed sea surface temperatures (SSTs), as demonstrated for MAGIC and COMBLE by Bogenschutz et al. (2025b). The latter permits atmospheric control of surface exchange but excludes feedbacks of the simulated surface energy budget on SST. Interactive land and ocean coupling share the objective of allowing the surface and atmosphere to evolve together; however, land feedbacks depend on soil moisture, soil temperature, and vegetation, whereas ocean feedbacks depend on heat storage and upper-ocean mixing. Coupled atmosphere–ocean SCMs, such as that of Hartung et al. (2018), explicitly represent these ocean responses. We currently have no plans to couple E3SM SCM or DP-SCREAM to a full ocean model, although a slab ocean could provide a comparatively simple future extension for examining thermodynamic feedbacks, subject to assumptions about mixed-layer depth and unresolved ocean heat transport.

Code and data availability. Code, data, and model output used in this study can be found at Bogenschutz (2026) (https://doi.org/10.5281/zenodo.20549582, last access: 5 June 2026).

Author contributions. PB and YZ conceived of the study. PB developed the capability to run E3SM SCM and DP-SCREAM with interactive land model and performed the simulations. HYM assisted with the generation of the initial condition files for the land model. PB, YZ, and HYM assisted with the interpretation of the results. CT and SX assisted with the processing of ARMBE data and providing variational reanalysis for the simulations performed in this work. YZ secured the project funding. All co-authors contributed to the manuscript.

Competing interests. The contact author has declared that none of the authors has any competing interests.

Acknowledgements. This research was primarily supported by the Atmospheric System Research program, Tying in High Resolution E3SM with ARM Data (THREAD) project (SCW1800) (P. Bogenschutz, Y. Zhang, and H.-Y. Ma) and partially supported by the Atmospheric Radiation Measurement (ARM) program (C. Tao and S. Xie), funded by the U.S. Department of Energy (DOE), Office of Science, Office of Biological and Environmental Research.

Work at LLNL was performed under the auspices of the U.S. DOE by Lawrence Livermore National Laboratory under contract DE-AC52-07NA27344. IM release number: LLNL-JRNL-2020166.

References

Anber, U., Gentine, P., Wang, S., and Sobel, A. H.: Fog and rain in the Amazon, Proceedings of the National Academy of Sciences, 112, 11 473–11 477, https://doi.org/10.1073/pnas.1505077112, 2015.

Bernard, E., Roehrig, R., Couvreux, F., Canut, G., Delire, C., Lohou, F., Lothon, M., and Decharme, B.: Process-Level Evaluation of the Land-Atmosphere Interactions Within CNRM-CM6-1 Single-Column Model Configuration, Journal of Advances in Modeling Earth Systems, 17, e2025MS005 090, https://doi.org/10.1029/2025MS005090, 2025.

Betts, A. K.: Understanding hydrometeorology using global models, Bulletin of the American Meteorological Society, 85, 1673–1688, https://doi.org/10.1175/BAMS-85-11-1673, 2004.

Bogenschutz, P.: Code and Data for "Interactive Land in E3SM Process-Level Models: Impacts of Land–Atmosphere Coupling in SCM and DP-SCREAM" [Data set]., https://doi.org/10.5281/zenodo.20549582, 2026.

Bogenschutz, P. A. and Krueger, S. K.: A simplified PDF parameterization of subgrid-scale clouds and turbulence for cloud-resolving models, Journal of Advances in Modeling Earth Systems, 5, 195–211, https://doi.org/https://doi.org/10.1002/jame.20018, 2013.

Bogenschutz, P. A., Gettelman, A., Morrison, H., Larson, V. E., Craig, C., and Schanen, D. P.: Higher-Order Turbulence Closure and Its Impact on Climate Simulations in the Community Atmosphere Model, Journal of Climate, 26, 9655–9676, https://doi.org/10.1175/JCLI-D-13-00075.1, 2013.

Bogenschutz, P. A., Tang, S., Caldwell, P. M., Xie, S., Lin, W., and Chen, Y.-S.: The E3SM version 1 single-column model, Geoscientific Model Development, 13, 4443–4458, https://doi.org/10.5194/gmd-13-4443-2020, 2020.

Bogenschutz, P. A., Eldred, C., and Caldwell, P. M.: Horizontal Resolution Sensitivity of the Simple Convection-Permitting E3SM Atmosphere Model in a Doubly-Periodic Configuration, Journal of Advances in Modeling Earth Systems, 15, e2022MS003 466, https://doi.org/https://doi.org/10.1029/2022MS003466, e2022MS003466 2022MS003466, 2023.

Bogenschutz, P. A., Clevenger, T. C., Bradley, A., Caldwell, P. M., Beydoun, H., Mahfouz, N., Keen, N. D., Guba, O., Bertagna, L., Foucar, J. G., Zhang, J., and Donahue, A. S.: High Performance, High Fidelity: A GPU-Accelerated Doubly-Periodic Version of the Simple Cloud-Resolving E3SM Atmosphere Model Version 1 (DP-SCREAMv1), ESS Open Archive, https://doi.org/10.22541/essoar.173655643.33295443/v1, preprint, submitted April 15, 2025; published April 22, 2025, 2025a.

Bogenschutz, P. A., Zhang, Y., Zheng, X., Tian, Y., Zhang, M., Lin, L., Wu, P., Xie, S., and Tao, C.: Exposing Process-Level Biases in a Global Cloud Permitting Model With ARM Observations, Journal of Geophysical Research: Atmospheres, 130, e2024JD043 059, https://doi.org/https://doi.org/10.1029/2024JD043059, e2024JD043059 2024JD043059, 2025b.

Bosveld, F. C., Baas, P., Steeneveld, G.-J., Holtslag, A. A. M., Angevine, W. M., Bazile, E., de Bruijn, E. I. F., Deacu, D., Edwards, J. M., Ek, M., Larson, V. E., Pleim, J. E., Raschendorfer, M., and Svensson, G.: The Third GABLS Intercomparison Case for Evaluation Studies of Boundary-Layer Models. Part B: Results and Process Understanding, Boundary-Layer Meteorology, 152, 157–187, https://doi.org/10.1007/s10546-014-9919-1, 2014.

Donahue, A. S., Caldwell, P. M., Bertagna, L., Beydoun, H., Bogenschutz, P. A., Bradley, A. M., Clevenger, T. C., Foucar, J., Golaz, C., Guba, O., Hannah, W., Hillman, B. R., Johnson, J. N., Keen, N., Lin, W., Singh, B., Sreepathi, S., Taylor, M. A., Tian, J., Terai, C. R., Ullrich, P. A., Yuan, X., and Zhang, Y.: To Exascale and Beyond—The Simple Cloud-Resolving E3SM Atmosphere Model (SCREAM), a Performance Portable Global Atmosphere Model for Cloud-Resolving Scales, Journal of Advances in Modeling Earth Systems, 16, e2024MS004 314, https://doi.org/https://doi.org/10.1029/2024MS004314, e2024MS004314 2024MS004314, 2024.

Gettelman, A., Truesdale, J. E., Bacmeister, J. T., Caldwell, P. M., Neale, R. B., Bogenschutz, P. A., and Simpson, I. R.: The Single Column Atmosphere Model Version 6 (SCAM6): Not a Scam but a Tool for Model Evaluation and Development, Journal of Advances in Modeling Earth Systems, 11, 1381–1401, https://doi.org/https://doi.org/10.1029/2018MS001578, 2019.

Ghan, S., Randall, D., Xu, K.-M., Cederwall, R., Cripe, D., Hack, J., Iacobellis, S., Klein, S., Krueger, S., Lohmann, U., Pedretti, J., Robock, A., Rotstayn, L., Somerville, R., Stenchikov, G., Sud, Y., Walker, G., Xie, S., Yio, J., and Zhang, M.: A Comparison of Single Column Model Simulations of Summertime Midlatitude Continental Convection, Journal of Geophysical Research: Atmospheres, 105, 2091–2124, https://doi.org/10.1029/1999JD900971, 2000.

Golaz, J.-C., Larson, V. E., and Cotton, W. R.: A PDF-Based Model for Boundary Layer Clouds. Part I: Method and Model Description, Journal of the Atmospheric Sciences, 59, 3540–3551, https://doi.org/10.1175/1520-0469(2002)059<3540:APBMFB>2.0.CO;2, 2002.

Golaz, J.-C., Caldwell, P. M., Roekel, L. P. V., Petersen, M. R., Tang, Q., Wolfe, J. D., and Co-authors: The DOE E3SM coupled model version1: Overview and evaluation at standard resolution, J. Adv. Model. Earth Syst., in press, https://doi.org/https://doi.org/10.1029/2018MS001603, 2019.

Golaz, J.-C., Lin, W., Zheng, X., Xie, S., Roberts, A. F., Van Roekel, L. P., Thornton, P. E., Barthel, A. M., Bradley, A. M., Wolfe, J. D., Zhang, C., Zhang, K., Zhang, S., Asay-Davis, X. S., Begeman, C. B., Bisht, G., Burrows, S. M., Chen, C.-C.-J., Feng, Y., Hunke, E. C., Jacob, R. L., Ke, Z., Mahajan, S., Mahfouz, N. G., Maltrud, M. E., Shi, X., Tang, Q., Terai, C. R., Thomas, E. E., Wang, H., Xie, J., Zhou, T., Bartoletti, T., Benedict, J. J., Brunke, M. A., Comeau, D. S., Fan, J., Forsyth, R. M., Foucar, J. G., Guba, O., Hannah, W. M., Hao, D., Huang, X., Jeffery, N., Kang, H.-G., Keen, N. D., Lee, H.-H., Lee, J., Liu, X., Mametjanov, A., Muelmenstaedt, J., Petersen, M. R., Prather, M. J., Price, S. F., Qian, Y., Salinger, A. G., Santos, S. P., Shan, Y., Singh, B., Smith, K. M., Song, X., Sreepathi, S., Turner, A. K., Vo, T., Wan, H., Wu, M., Yu, W., Zender, C. S., Zeng, X., Zhang, G. J., Zhang, M., Zhang, T., Zhang, Y., McCoy, R. B., Taylor, M. A., Leung, L. R., Caldwell, P. M., and Bader, D. C.: The Energy Exascale Earth System Model Version 3: 2. Overview of the Coupled System, Journal of Advances in Modeling Earth Systems, 18, e2025MS005 302, https://doi.org/https://doi.org/10.1029/2025MS005302, e2025MS005302 2025MS005302, 2026.

Hartung, K., Svensson, G., Struthers, H., Deppenmeier, A.-L., and Hazeleger, W.: An EC-Earth coupled atmosphere–ocean single-column model (AOSCM.v1$_{E}C-Earth3)forstudyingcoupledmarineandpolarprocesses, GeoscientificModelDevelopment, 11, 4117--4137,$ https://doi.org/$10.5194/gmd-11-4117-2018, 2018$.

Hersbach, H., Bell, B., Berrisford, P., Hirahara, S., Horányi, A., Muñoz-Sabater, J., Nicolas, J., Peubey, C., Radu, R., Schepers, D., Simmons, A., Soci, C., Abdalla, S., Abellan, X., Balsamo, G., Bechtold, P., Biavati, G., Bidlot, J., Bonavita, M., De Chiara, G., Dahlgren, P., Dee, D., Diamantakis, M., Dragani, R., Flemming, J., Forbes, R., Fuentes, M., Geer, A., Haimberger, L., Healy, S., Hogan, R. J., Hólm, E., Janisková, M., Keeley, S., Laloyaux, P., Lopez, P., Lupu, C., Radnoti, G., de Rosnay, P., Rozum, I., Vamborg, F., Villaume, S., and Thépaut, J.-N.: The ERA5 global reanalysis, Quarterly Journal of the Royal Meteorological Society, 146, 1999–2049, https://doi.org/https://doi.org/10.1002/qj.3803, 2020.

Khairoutdinov, M. F. and Randall, D. A.: Cloud Resolving Modeling of the ARM Summer 1997 IOP: Model Formulation, Results, Uncertainties, and Sensitivities, Journal of the Atmospheric Sciences, 60, 607 – 625, https://doi.org/10.1175/1520-0469(2003)060<0607:CRMOTA>2.0.CO;2, 2003.

Lawrence, D. M., Oleson, K. W., Flanner, M. G., Thornton, P. E., Swenson, S. C., Lawrence, P. J., Zeng, X., Yang, Z.-L., Levis, S., Sakaguchi, K., Bonan, G. B., and Slater, A. G.: Parameterization Improvements and Functional and Structural Advances in Version 4 of the Community Land Model (CLM4), Journal of Advances in Modeling Earth Systems, 3, M03 001, https://doi.org/10.1029/2011MS000045, 2011.

Lee, J. M. and Khairoutdinov, M.: A Simplified Land Model (SLM) for use in cloud-resolving models: Formulation and evaluation, Journal of Advances in Modeling Earth Systems, 7, 1368–1392, https://doi.org/https://doi.org/10.1002/2014MS000419, 2015.

Lombardozzi, D. L., Lu, Y., Lawrence, D. M., Lawrence, P. J., Swenson, S. C., Wieder, W. R., Ainsworth, E. A., Bonan, G. B., Fisher, R. A., Levis, S., and Xu, C.: Description and Evaluation of Implementation of Plant Hydraulics in the Community Land Model, Version 5, Journal of Advances in Modeling Earth Systems, 12, e2019MS001 841, https://doi.org/10.1029/2019MS001841, 2020.

Martin, S. T., Artaxo, P., Machado, L. A. T., Manzi, A. O., Souza, R. A. F., Schumacher, C., Wang, J., Andreae, M. O., Barbosa, H. M. J., Fan, J., Fisch, G., Goldstein, A. H., Guenther, A., Jimenez, J. L., Kuang, C., Liao, H., McKinney, K. A., Medeiros, A., Prohaska, N., Rizzo, L. V., Sachs, J., Tota, J., Silva Dias, M. A. F., Smith, J. N., Springston, S. R., Souza, E. F., and Wendisch, M.: The Green Ocean Amazon Experiment (GoAmazon2014/5) Observes Pollution Affecting Gases, Aerosols, Clouds, and Rainfall over the Rain Forest, Bulletin of the American Meteorological Society, 98, 981–997, https://doi.org/10.1175/BAMS-D-15-00221.1, 2017.

Mather, J. H. and Voyles, J. W.: The ARM Climate Research Facility: A Review of Structure and Capabilities, Bulletin of the American Meteorological Society, 94, 377–392, https://doi.org/10.1175/BAMS-D-11-00218.1, 2013.

Morrison, H. and Milbrandt, J. A.: Parameterization of Cloud Microphysics Based on the Prediction of Bulk Ice Particle Properties. Part I: Scheme Description and Idealized Tests, Journal of the Atmospheric Sciences, 72, 287 – 311, https://doi.org/10.1175/JAS-D-14-0065.1, 2015.

Morrison, H., Milbrandt, J. A., Bryan, G. H., Ikeda, K., Tessendorf, S. A., and Thompson, G.: Parameterization of Cloud Microphysics Based on the Prediction of Bulk Ice Particle Properties. Part II: Case Study Comparisons with Observations and Other Schemes, Journal of the Atmospheric Sciences, 72, 312 – 339, https://doi.org/10.1175/JAS-D-14-0066.1, 2015.

Oware, R. K. T., Zheng, Y., Bogenschutz, P., Zhang, Y., Ma, H.-Y., Xie, S., and Tao, C.: Evaluating E3SM Global Storm-Resolving Model Simulations of Deep Convection: Insights From DP-SCREAM During TRACER, Journal of Geophysical Research: Atmospheres, 130, e2025JD044 113, https://doi.org/https://doi.org/10.1029/2025JD044113, e2025JD044113 2025JD044113, 2025.

Santanello, J. A., Dirmeyer, P. A., Ferguson, C. R., Findell, K. L., Tawfik, A. B., Berg, A., Ek, M., Gentine, P., Guillod, B. P., van Heerwaarden, C. C., Roundy, J., and Wulfmeyer, V.: Land–Atmosphere Interactions: The LoCo Perspective, Bulletin of the American Meteorological Society, 99, 1253–1272, https://doi.org/10.1175/BAMS-D-17-0001.1, 2018.

Shan, Y., Liu, X., Lin, L., Ke, Z., Lu, Z., Tilmes, S., Gao, L., and Yu, P.: The Role of In-Cloud Wet Removal in Simulating Aerosol Vertical Profiles and Cloud Radiative Forcing, Journal of Geophysical Research: Atmospheres, 128, e2023JD038 564, https://doi.org/https://doi.org/10.1029/2023JD038564, e2023JD038564 2023JD038564, 2023.

Song, X., Zhang, G., Wan, H., and Xie, S.: Incorporating the Effect of Large-Scale Vertical Motion on Convection Through Convective Mass Flux Adjustment in E3SMv2, Journal of Advances in Modeling Earth Systems, 15, e2022MS003 553, https://doi.org/https://doi.org/10.1029/2022MS003553, e2022MS003553 2022MS003553, 2023.

Song, X., Zhang, G. J., Terai, C., and Xie, S.: Enhanced Convective Microphysics Scheme and Its Impacts on Mean Climate in E3SM, Journal of Advances in Modeling Earth Systems, 17, e2024MS004 656, https://doi.org/https://doi.org/10.1029/2024MS004656, e2024MS004656 2024MS004656, 2025.

Tang, S., Xie, S., Zhang, Y., Zhang, M., Schumacher, C., Upton, H., Jensen, M. P., Johnson, K. L., Wang, M., Ahlgrimm, M., Feng, Z., Minnis, P., and Thieman, M.: Large-scale vertical velocity, diabatic heating and drying profiles associated with seasonal and diurnal variations of convective systems observed in the GoAmazon2014/5 experiment, Atmospheric Chemistry and Physics, 16, 14 249–14 264, https://doi.org/10.5194/acp-16-14249-2016, 2016.

Tang, S., Xie, S., Guo, Z., Hong, S.-Y., Khouider, B., Klocke, D., Köhler, M., Koo, M.-S., Krishna, P. M., Larson, V. E., Park, S., Vaillancourt, P. A., Wang, Y.-C., Yang, J., Daleu, C. L., Homeyer, C. R., Jones, T. R., Malap, N., Neggers, R., Prabhakaran, T., Ramirez, E., Schumacher, C., Tao, C., Bechtold, P., Ma, H.-Y., Neelin, J. D., and Zeng, X.: Long-term single-column model intercomparison of diurnal cycle of precipitation over midlatitude and tropical land, Quarterly Journal of the Royal Meteorological Society, 148, 641–669, https://doi.org/https://doi.org/10.1002/qj.4222, 2022.

Terai, C. R., Xie, S., Song, X., Chen, C.-C., Fan, J., Zhang, G. J., Richter, J. H., Shpund, J., Lin, W., Golaz, J.-C., Larson, V. E., Moncrieff, M. W., Shan, Y., Zhang, C., Zhang, K., and Zhang, Y.: Impact of Microphysics and Convection Schemes on the Mean-State and Variability of Clouds and Precipitation in the E3SM Atmosphere Model, Journal of Advances in Modeling Earth Systems, 17, e2024MS004 569, https://doi.org/https://doi.org/10.1029/2024MS004569, e2024MS004569 2024MS004569, 2025.

Tian, J., Zhang, Y., Klein, S. A., Terai, C. R., Caldwell, P. M., Beydoun, H., Bogenschutz, P., Ma, H.-Y., and Donahue, A. S.: How Well Does the DOE Global Storm Resolving Model Simulate Clouds and Precipitation Over the Amazon?, Geophysical Research Letters, 51, e2023GL108 113, https://doi.org/https://doi.org/10.1029/2023GL108113, e2023GL108113 2023GL108113, 2024.

Tian, Y. and Zhang, Y.: Factors Controlling Precipitation Onset and Maintenance: Inferences from Large Eddy Simulations of Two Afternoon Deep Convective Regimes over Amazon, Geophysical Research Letters, https://doi.org/https://doi.org/10.1029/2024GL113920, 2025.

Xie, S., Cederwall, R. T., and Zhang, M.: Developing long-term single-column model/cloud system–resolving model forcing data using numerical weather prediction products constrained by surface and top of the atmosphere observations, Journal of Geophysical Research: Atmospheres, 109, https://doi.org/https://doi.org/10.1029/2003JD004045, 2004.

Xie, S., McCoy, R., Klein, S. A., Cederwall, R. T., Wiscombe, W. J., Clothiaux, E. E., Gaustad, K. L., Golaz, J.-C., Hall, S. D., Jensen, M. P., Johnson, K. L., Lin, Y., Long, C. N., Mather, J. H., McCord, R. A., McFarlane, S. A., Palanisamy, G., Shi, Y., and Turner, D. D.: Clouds and More: ARM Climate Modeling Best Estimate Data: A New Data Product for Climate Studies, Bulletin of the American Meteorological Society, 91, 13–20, https://doi.org/10.1175/2009BAMS2891.1, 2010.

Xie, S., Terai, C. R., Wang, H., Tang, Q., Fan, J., Burrows, S., Lin, W., Wu, M., Song, X., Zhang, Y., Taylor, M. A., Golaz, J.-C., Benedict, J. J., Chen, C.-C.-J., Feng, Y., Hannah, W. M., Ke, Z., Shan, Y., Larson, V. E., Liu, X., Prather, M. J., Richter, J. H., Shrivastava, M., Wan, H., Zhang, G. J., Zhang, K., Bradley, A. M., Cameron-Smith, P., Damiano, L., Debusschere, B. J., Donahue, A. S., Easter, R. C., Eldred, M. S., Griffin, B. M., Guba, O., Guo, Z., Huang, X., Lee, J., Lee, H.-H., Lou, S., Mahfouz, N., Moncrieff, M., Mülmenstädt, J., Qian, Y., Rasool, Q. Z., Roberts, A. F., Santos, S. P., Sargsyan, K., Shpund, J., Singh, B., Tao, C., Xie, J., Yang, Y., Zeng, X., Zhang, C., Zhang, M., Zhang, S., Zhang, T., Zheng, X., Jacob, R. L., Leung, L. R., McCoy, R. B., and Bader, D. C.: The Energy Exascale Earth System Model Version 3: 1. Overview of the Atmospheric Component, Journal of Advances in Modeling Earth Systems, 17, e2025MS005 120, https://doi.org/https://doi.org/10.1029/2025MS005120, e2025MS005120 2025MS005120, 2025.

Zhang, G. and McFarlane, N. A.: Sensitivity of climate simulations to the parameterization of cumulus convection in the Canadian climate centre general circulation model, Atmosphere-Ocean, 33, 407–446, https://doi.org/10.1080/07055900.1995.9649539, 1995.

Zhang, M. H., Lin, J. L., Cederwall, R. T., Yio, J. J., and Xie, S. C.: Objective Analysis of ARM IOP Data: Method and Sensitivity, Monthly Weather Review, 129, 295 – 311, https://doi.org/10.1175/1520-0493(2001)129<0295:OAOAID>2.0.CO;2, 2001.

Zhang, Y., Klein, S. A., Fan, J., Chandra, A. S., Kollias, P., Xie, S., and Tang, S.: Large-Eddy Simulation of Shallow Cumulus over Land: A Composite Case Based on ARM Long-Term Observations at Its Southern Great Plains Site, Journal of the Atmospheric Sciences, 74, 3229 – 3251, https://doi.org/10.1175/JAS-D-16-0317.1, 2017.